Geoscience Frontiers xxx (2014) 1–18

Contents lists available at ScienceDirect

China University of Geosciences (Beijing)

Geoscience Frontiers

journal homepage: www.elsevier.com/locate/gsf

Research paper

Tectonically asymmetric Earth: From net rotation to polarized westward drift of the lithosphere

Carlo Doglioni [a], Eugenio Carminati [a], Mattia Crespi [b], Marco Cuffaro [c,*], Mattia Penati [d], Federica Riguzzi [e]

[a] Dipartimento di Scienze della Terra, Sapienza Università di Roma, Rome, Italy
[b] DITS – Area di Geodesia e Geomatica, Sapienza Università di Roma, Rome, Italy
[c] Istituto di Geologia Ambientale e Geoingegneria, CNR, Rome, Italy
[d] MOX – Dipartimento di Matematica, Politecnico di Milano, Milan, Italy
[e] Istituto Nazionale di Geofisica e Vulcanologia, Sez. CNT, Rome, Italy

ARTICLE INFO

Article history:
Received 14 October 2013
Received in revised form
23 January 2014
Accepted 6 February 2014
Available online xxx

Keywords:
Asymmetric plate tectonics
Plate motions
Westward drift
Mantle convection

ABSTRACT

The possibility of a net rotation of the lithosphere with respect to the mantle is generally overlooked since it depends on the adopted mantle reference frames, which are arbitrary. We review the geological and geophysical signatures of plate boundaries, and show that they are markedly asymmetric worldwide. Then we compare available reference frames of plate motions relative to the mantle and discuss which is at best able to fit global tectonic data. Different assumptions about the depths of hotspot sources (below or within the asthenosphere, which decouples the lithosphere from the deep mantle) predict different rates of net rotation of the lithosphere relative to the mantle. The widely used no-net-rotation (NNR) reference frame, and low (<0.2°–0.4°/Ma) net rotation rates (deep hotspots source) predict an average net rotation in which some plates move eastward relative to the mantle (e.g., Nazca). With fast (>1°/Ma) net rotation (shallow hotspots source), all plates, albeit at different velocity, move westerly along a curved trajectory, with a tectonic equator tilted about 30° relative to the geographic equator. This is consistent with the observed global tectonic asymmetries.

1. Introduction

The driving mechanism of plate tectonics is still controversial. The classic view is that plates are simply the tops of large convection cells. The top-down, or plate model, attributes mantle convection to the motions of plates and slabs, which, in turn, are a consequence of secular cooling of the Earth modulated by internal heating. A third view is that active narrow plumes from the core mantle boundary drive the plates. The role of a low-viscosity zone, or asthenosphere, is invoked in all models.

A basic step in the geodynamic modelling of plate tectonics consists in the choice of the reference frame and of plate velocities as boundary conditions. If plate motions with respect to the deep mantle (Morgan, 1971; Wilson, 1973) could be determined, this would represent the most direct way to infer the causes of plate tectonic motions. A common assumption in geodynamics is that plate motions are driven by mantle and lithosphere heterogeneities and mantle convection (e.g., Tackley, 2000a). Several authors claim that plates are driven primarily by "slab pull", i.e., by the negative buoyancy of slabs (e.g., Conrad and Lithgow-Bertelloni, 2002). However, relative plate velocities and slab dip are not related to the age of the downgoing lithosphere (Cruciani et al., 2005) and some plates move without an attached slab (Doglioni et al., 2007). Of course, plates are a mosaic and their motions are controlled by adjacent plates, as well as by forces that are created by attached slabs. Conrad and Lithgow-Bertelloni (2002) proposed trench suction as the dominant mechanism for moving plates such as South

* Corresponding author. Istituto di Geologia Ambientale e Geoingegneria (IGAG), CNR, c/o Dipartimento di Scienze della Terra, Sapienza Università di Roma, P.le A. Moro 5, I-00185 Rome, Italy. Tel.: +39 06 4991 4575; fax: +39 06 4454729.
E-mail address: marco.cuffaro@igag.cnr.it (M. Cuffaro).

Peer-review under responsibility of China University of Geosciences (Beijing)

Production and hosting by Elsevier

1674-9871/$ – see front matter © 2014, China University of Geosciences (Beijing) and Peking University. Production and hosting by Elsevier B.V. All rights reserved.
http://dx.doi.org/10.1016/j.gsf.2014.02.001

America that do not have large sections of attached slabs. However there are plates such as Africa or Eurasia that move without slabs in their direction of motion and, in these cases, the trench suction model does not apply.

Cenozoic magnetic anomalies and the trend of subduction zones indicate that plates follow globally coherent trajectories (Doglioni, 1990). Deviations from this global flow have been ascribed to plate subrotations (Cuffaro et al., 2008), a phenomenon frequently invoked for microplates, and the effects of adjacent plates. GPS data of the last decades have shown that plates now move at speeds and trends quite similar to those of the geologic past (based on magnetic anomalies and subduction zones age constraints), confirming the existence of a sort of "tectonic equator" inclined about 30° with respect to the geographic equator (Crespi et al., 2007).

Moreover, since the early studies of Morgan (1971) and Wilson (1973), it was proposed that the lithosphere is moving relative to the underlying mantle. Volcanic tracks, shear wave splitting, the recognition of the low-velocity layer or zone (LVZ), support the notion that the lithosphere is decoupled relative to the underlying mantle, being the LVZ in the upper asthenosphere the shear boundary layer. Moreover, this decoupling appears polarized. In fact models with a net "westerly" directed rotation of the lithosphere relative to the mantle were provided by a number of articles (e.g., Le Pichon, 1968; Bostrom, 1971; Nelson and Temple, 1972; Moore, 1973; Shaw, 1973; O'Connell et al., 1991; Ricard et al., 1991). It is worth noting that the mean net rotation is consistently close or overlapping the tectonic equator (Crespi et al., 2007; Cuffaro and Doglioni, 2007), indirectly supporting its existence and significance. For the uncertainty on the shape and location of the tectonic equator see Crespi et al. (2007).

Since the hotspots reference frame is crucial for measuring the net rotation of the lithosphere, the source and reliability of hotspots is crucial. However some questions about hotspots remain unresolved, such as the correct number of seamount track to use for the definition of the framework, or the choice of their source depth (Bonatti, 1990; Norton, 2000; Doglioni et al., 2005; Foulger et al., 2005) and whether only trends, not ages, should be used (Morgan and Phipps Morgan, 2007). Nonetheless, the hotspot reference frame continues to be a convenient – and easy to visualize – framework in which to study plate kinematics and dynamics. Many absolute present-day plate kinematic models have been proposed incorporating plate motions from magnetic anomalies (O'Connell et al., 1991; Wang and Wang, 2001; Gripp and Gordon, 2002; Cuffaro and Doglioni, 2007) and geodetic data (Crespi et al., 2007) into the hotspot frame. In other models, plate motions and plate reconstructions were attempted for the past (Gordon and Jurdy, 1986; Müller et al., 1993; Steinberger et al., 2004; O'Neill et al., 2005; Torsvik et al., 2010). All these absolute plate motions imply a net rotation of the lithosphere, corresponding to an average rotation of the Earth's surface considered as a whole, indicating an implicit westward drift of the lithosphere, albeit with different magnitudes and poles of rotation. The toroidal-poloidal partitioning of plate motions was found to be larger than expect (e.g., O'Connell et al., 1991; Tackley, 2000b).

Although the net rotation is a recognized feature, its magnitude is uncertain owing to a large variability of constraints that need to be assumed, e.g., the number of hotspots used (Ricard et al., 1991; Gripp and Gordon, 2002), the velocity of the Pacific plate (Zheng et al., 2010), the depth of the source for the hotspots, the use of intraplate hotsposts only (Doglioni et al., 2005; Crespi et al., 2007; Cuffaro and Doglioni, 2007), alternative to the use of near and on plate boundary hotspots (Doubrovine et al., 2012). Slow net rotation models come from hotspot reference frames in which all volcanic trails are used regardless they are both intraplate and near ridge. Moreover these models consider the source of the plumes deeply rooted (base of the lower mantle). Fast net rotation models are instead based on a discrimination of "hotspots", removing those which are located along ridges or transform faults, and generating volcanic tracks without any relation with the plate boundaries (i.e., the Pacific hotspots). In addition, if the source of hotspots is alternatively assumed to be deep (lowermost mantle) or shallow (intra-low-velocity zone [LVZ] source), slow and fast net rotations are predicted, respectively. Based on the recent petrologic and seismological studies indicating an asthenospheric source of Hawaii OIB (e.g., Anderson, 2011; Presnall and Gudfinnsson, 2011; Rychert et al., 2013), a shallow-hotspot class of models can be envisaged, in which the faster westward net rotation is a consequence that the source of the hotspots is located in the middle of the decoupling zone (somewhere between 100 and 250 km depth, Doglioni et al., 2005; Cuffaro and Doglioni, 2007). Consequently, the volcanic track at the surface records only the relative motion of the lithosphere from the source depth, disregarding the part of decoupling below it. Most of the disagreement on the source depth of hotspots (i.e., deep, at the core-mantle boundary, or shallow, within the asthenosphere) derives from a series of circular reasonings and tomographic interpretations. However, relative mantle tomography is often biased by a number of assumptions (see Foulger et al., 2013).

Some geodynamic models, alternative to purely kinematic models, predicted different net rotations of the lithosphere (e.g., Zhong, 2001). Analysing seismic anisotropy Becker (2006), Kreemer (2009), Conrad and Behn (2010) found that the net rotation should be, at most, 50% of that obtained by Gripp and Gordon (2002) with model HS3-NUVEL1A, that proposes the highest net rotation value among the well-accepted absolute plate kinematic models relative to the hotspots. The argument of Conrad and Behn (2010) is that the reference frame of Gripp and Gordon (2002) is based on the fastest moving plates in the Pacific. However, most hotspots reference frames use indiscriminately volcanic tracks. Several hotspots used in other reference frames are located near ridges or transform faults (e.g., Atlantic and Indian oceans), plate boundaries which are by definition moving relative to each other and relative to the mantle (e.g., Le Pichon, 1968). In fact many of those volcanic tracks have been shown to be superficial and related to a mantle richer in fluids which lower the melting temperature (e.g., Bonatti, 1990), and the reconstruction of past evolution shows that the Indo-Atlantic hotspots moved relative to the pacific ones (e.g., Doubrovine et al., 2012). Pacific volcanic chains (e.g., Hawaii) are rather intraplate and independent to plate boundaries; therefore they better represent the motion of the plate with respect to the mantle source. On the other hand, Alpert et al. (2010), in their model, obtained that high values of net rotation of the lithosphere provide accurate agreement with slab deformation, as also proposed by Doglioni et al. (2007).

Torsvik et al. (2010) computed the net rotation of the lithosphere (using indiscriminately all the hotspots and assuming that they are sourced from the deep mantle) and found that it is very slow, and that it has varied over the past 150 Ma. In their opinion this could suggest that the net rotation has tectonic origins, and does not result from a continuous external forcing (i.e., tidal drag). However, a non random distribution of paleopoles of rotation during the last 600 Ma has been observed (Vérard et al., 2012), supporting a rotational tuning of plate tectonics throughout the Earth's history (Doglioni, 1990; Scoppola et al., 2006; Riguzzi et al., 2010). Moreover, the combination of the presence of low viscosity rocks in the asthenosphere (Doglioni et al., 2011), the polarized westward drift of the lithosphere controlling an asymmetric pattern of mantle convection, and the available total amount of energy due to rotation and tides (Riguzzi et al., 2010), can suggest a global dynamics in which Earth's thermal cooling and astronomical forces coexist.

Please cite this article in press as: Doglioni, C., et al., Tectonically asymmetric Earth: From net rotation to polarized westward drift of the lithosphere, Geoscience Frontiers (2014), http://dx.doi.org/10.1016/j.gsf.2014.02.001

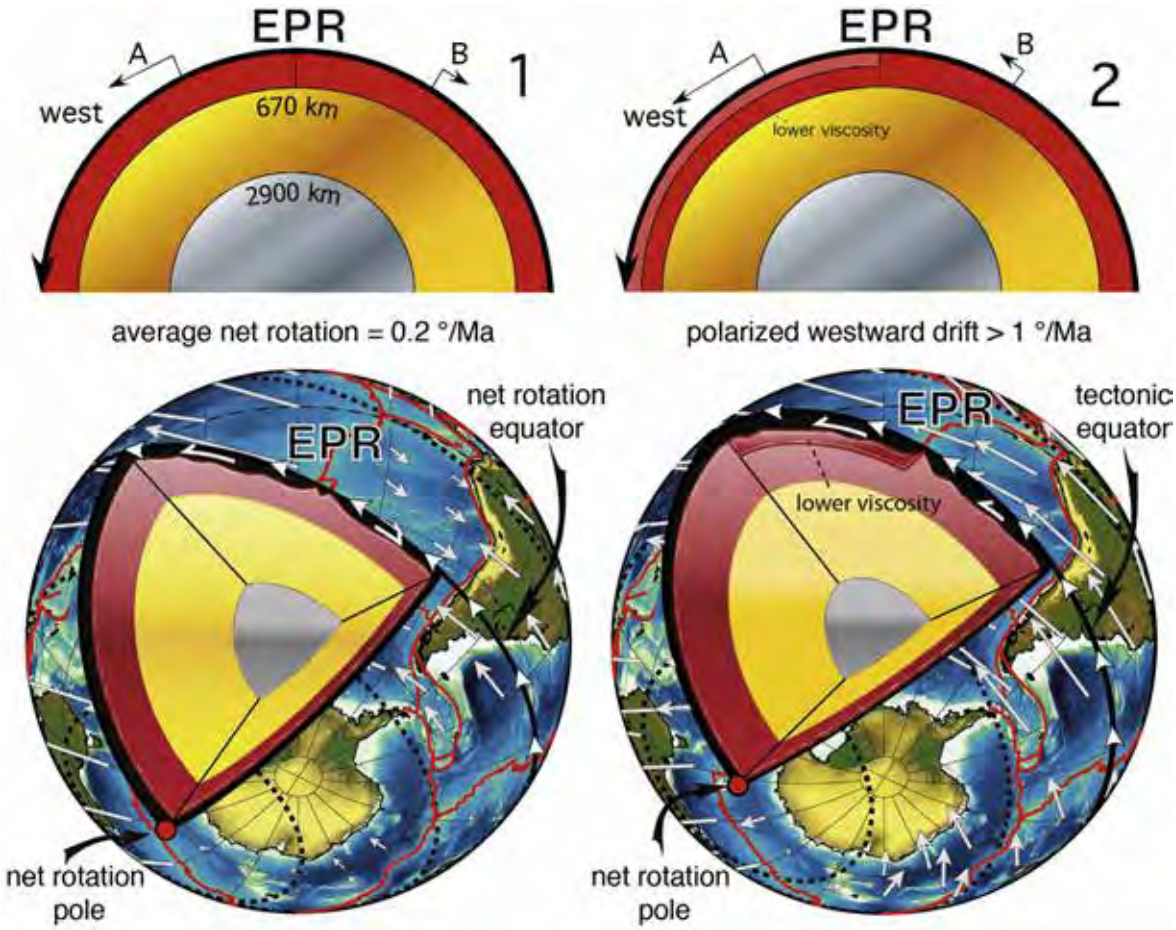

Figure 1. Plate kinematics across the East Pacific Rise (EPR) with respect to Pacific hotspots, with average low net rotation = 0.2°/Ma (1 – left column), and > 1°/Ma (2 – right column) respectively. When the net rotation of the lithosphere is low, plates A (Pacific) and B (Nazca) move in opposite directions relative to the mantle (left upper panel), also if an average net rotation vector field is W-directed along small circles (dashed lines, left lower panel) of the net rotation pole (red point in the figure) with a maximum linear velocity computed on the net rotation equator (solid black line). On the contrary, when net rotation is high, plates A (Pacific) and B (Nazca) move both westerly relative to the mantle (right upper panel), suggesting a global and polarized westward drift of the lithosphere along a different net rotation equator (solid black line, right lower panel), that can be detected with the tectonic equator, and the small circles (dashed lines) of the net rotation pole (red point in the figure). Faster velocities may be related to lower viscosity layers.

In models where the net rotation of the lithosphere is predicted to be low (0.2°/Ma, 2–4 cm/yr at equatorial latitudes), all the plates move westward relative to the underlying mantle except for Cocos and Nazca plates. The Pacific and Nazca plates move in opposite directions (eastward), while the East Pacific Rise still move westward (Fig. 1), and the average net rotation velocity field is still W-directed along the small circles of the relative net rotation pole and equator. This was interpreted to be due to the larger weight in the computation of the Pacific plate, which is moving WNW-ward at fast rates, due to the particularly low viscosity of the underlying asthenosphere (Ricard et al., 1991).

On the contrary, when the net rotation is predicted to be fast (>1°/Ma, equivalent to >10 cm/yr at the equator), i.e., when using intra-decoupling (intra-LVZ) shallow source of plumes as obtained by Crespi et al. (2007) and Cuffaro and Doglioni (2007), all plates (including Cocos and Nazca) rather move westward relative to the mantle. These results suggest a globally polarized westward drift of the lithosphere along the net rotation equator, likely corresponding with the tectonic equator (Crespi et al., 2007), as shown in Fig. 1. Faster plate velocities with respect to the mantle may be related to lower viscosity in the underlying LVZ at the top of the asthenosphere (Doglioni et al., 2006, 2007). In particular, the degree of decoupling between lithosphere and asthenosphere could be mainly controlled by the thickness and viscosity of the asthenosphere, and the lateral variations in decoupling could control the variable velocity of the overlying lithosphere. In this view, plates would be more or less detached with respect to the mantle, as a function of the decoupling at their base (Doglioni et al., 2003; Cuffaro and Doglioni, 2007; Doglioni et al., 2011).

The worldwide asymmetries of plate tectonic features that will be described and discussed in the following are here interpreted as the consequence of a geodynamic scenario characterized by the westward drift of the lithosphere and a global pattern of plate motions on a preferred trajectory named tectonic equator in the literature (Doglioni, 1990, 1993; Crespi et al., 2007). Recently Gérault et al. (2012) proposed that the net rotation of the lithosphere is generated by the asymmetric position of ridges on the Earth's surface and the asymmetric slab dipping angle in the mantle. The tectonic equator was quantitatively obtained by Riguzzi et al. (2006), regardless the net rotation of the lithosphere, and it describes the flow of plates relative to the mantle. It undulates relative to the geographic equator, at an angle of about 30°. Crespi et al. (2007) incorporated space geodesy data into the hotspot framework with variable source depth, and they found that the best fit for the tectonic equator corresponds to net rotation great circle, with a pole located at 56.4°S and 136.7°E. The existence of a

Please cite this article in press as: Doglioni, C., et al., Tectonically asymmetric Earth: From net rotation to polarized westward drift of the lithosphere, Geoscience Frontiers (2014), http://dx.doi.org/10.1016/j.gsf.2014.02.001

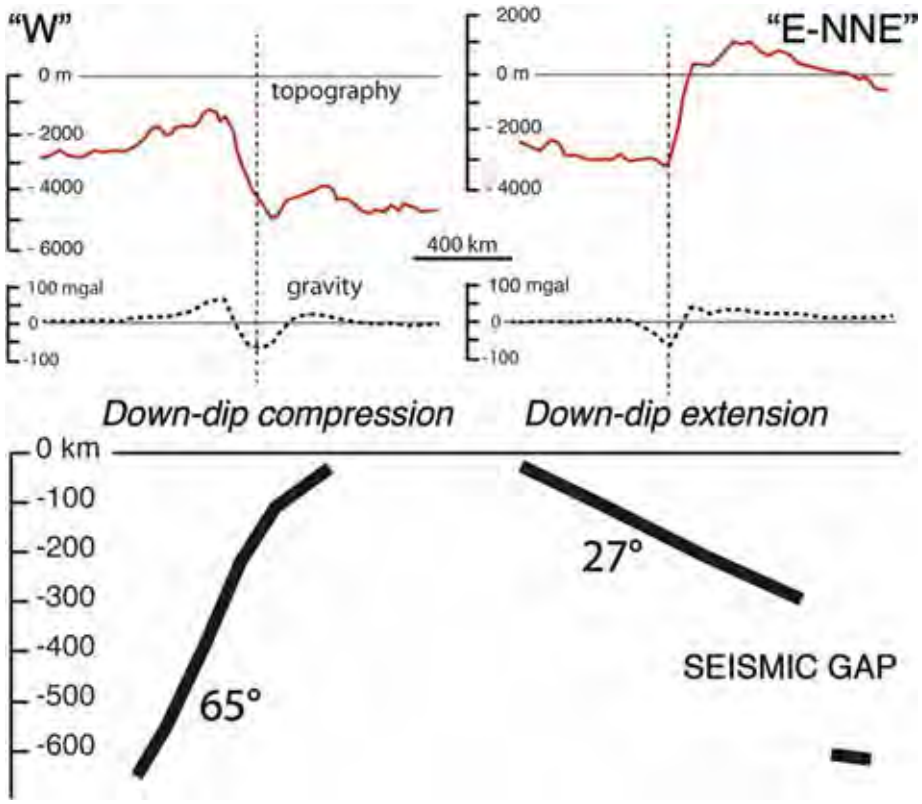

Figure 2. Upper panel – comparison between average topography (solid red line) and average free-air gravity anomaly (dashed black line) made at subduction zones, analysed by Harabaglia and Doglioni (1998), for W-directed subductions (left column) and E- and NE-directed ones (right column). Comparison shows that W-directed subduction zones are characterized by low-topography and E-directed ones by high topography, whereas they have higher amplitude gravity anomalies and lower one respectively. The higher gravity anomalies along the W-directed subduction zones reflect the occurrence of deeper trenches or foredeep basins (negative anomaly) and the mantle uplift in the backarc basin (positive anomaly), with respect to the opposite subduction zones where these two features are generally absent. Moreover, for the W-directed subduction, the minimum values for topography and gravity anomaly are shifted, considering the same length of the studied sections, whereas this shift does not occur for E- or NE-directed subductions. Lower panel – average slab dip, representing the mean trace of the seismicity along the subduction zones analysed by Riguzzi et al. (2010), for W-directed subduction (left column) and E- and NE-directed ones (right column). The W-directed slabs are, in average, dipping (65 ± 14)°, whereas the mean dip of the E- or NE-directed slabs is (27 ± 14)°. The asymmetry is also marked by the opposite behaviour of slab downgoing (down-dip compression and down-dip extension for W- and E- or NE- slab respectively; Doglioni et al., 2007), and by the seismic gap, around 300–550 km, occurring only along the E- or NE-directed subduction zones, that are, in general, shorter than the W-directed slabs.

global tectonic pattern (Doglioni, 1990, 1993) has been proposed in the literature based on geological and geophysical observables (Doglioni et al., 1999).

In this paper, we review and discuss worldwide asymmetries of plate tectonic features presenting, for the first time, projections of the main geophysical observables along the great circle describing the tectonic equator proposed by Crespi et al. (2007), as well along to two small circles (30°N and 30°S) of their net rotation pole, to get a direct and global view of asymmetric features pertaining to different geophysical data sets. The choice of plotting data along such great and circles depends on the fact that the obtained cross sections will be parallel to the absolute plate motion vector. Several previous analyses where made across plate boundaries parallel to the relative motion among two plates. We rather want to test here how the whole Earth is shaped when moving along the tectonic equator, i.e., following the first order motion of plates.

Since the net rotation implies a relative "eastward" sublithospheric mantle flow, its related geological and geophysical asymmetries should be maximum along the tectonic equator. In addition, we investigate the effects on absolute plate kinematics models of different assumptions (variable depth of the source) in the hotspot reference frame. Plate kinematic models with shallower hotspots sources predict more polarized westward plate motions, better explaining the asymmetric features of the Earth, with the underlying hypothesis that the lithosphere and the mantle are decoupled by an asthenosphere characterized by variable viscosity (Doglioni, 1993; Pollitz et al., 1998; Cuffaro and Doglioni, 2007). We finally discuss the consequences on mantle convection scenarios and propose a tentative explanation for global westward plate motions.

2. Tectonically asymmetric Earth: a literature perspective

A number of papers (Dickinson, 1978; Uyeda and Kanamori, 1979; Doglioni et al., 1999, 2007; Garzanti et al., 2007; Riguzzi et al., 2010) evidenced how subduction zones and related orogens are markedly asymmetric: W-directed subduction zones are steeper than those directed to E- or NE-, and the associated orogens are respectively characterized by lower structural and topographic elevation, occurrence of backarc basins, whereas E- or NE-directed subductions show higher structural and morphological elevation and no backarc basin. Harabaglia and Doglioni (1998) compared average topography and average free-air gravity anomalies of W-directed and E- and NE-directed subductions (Fig. 2). They found that W-directed subduction are characterized by low-topography and E-directed ones by high topography (−480 m vs. 1630 m mean maximum elevation, respectively), whereas they show higher and lower amplitude gravity anomalies respectively (259 mgal vs. 142 mgal). In fact, along W-directed subduction zones, there

Please cite this article in press as: Doglioni, C., et al., Tectonically asymmetric Earth: From net rotation to polarized westward drift of the lithosphere, Geoscience Frontiers (2014), http://dx.doi.org/10.1016/j.gsf.2014.02.001

regularly is a deep trench or foredeep (negative anomaly), and the slab is associated with the uplift of the mantle in the backarc basin (positive anomaly). Both features are missing in ongoing, "regular" (see discussion in Doglioni et al., 2007) E- or NE-directed subduction zones. Moreover, in W-directed subduction zones, the minimum values for topography is shifted with respect to the gravity anomaly (Fig. 2), while this shift does not occur for E- or NE-directed subductions. The average slab dip, representing the mean trace of the seismicity along the subduction zones, is 65° ± 15° in W-directed subductions and 27° ± 14° in E- or NE-directed slabs (Riguzzi et al., 2010). This asymmetry is also marked by the opposite state of stress of the slabs: down-dip compression and down-dip extension for W- and E- or NE- slab respectively (Doglioni et al., 2007; Carminati and Petricca, 2010). In addition, a seismic gap generally occurs at 300–550 km depth only along the E- or NE-directed subduction zones, that are, in general, shorter than the W-directed slabs (Fig. 2).

These asymmetries are striking when western and eastern Pacific subduction zones are compared. Such differences have usually been interpreted as related to the age of the downgoing oceanic lithosphere (usually older, cooler and denser in the western side). However these differences persist elsewhere, regardless of the age and composition of the downgoing lithosphere, e.g., in the Mediterranean Apennines and Carpathians vs. Alps and Dinarides, or in the Banda and Sandwich arcs, where even continental or zero-age oceanic (mid-oceanic ridge) lithosphere is almost vertical along W-directed subduction zones (Doglioni et al., 1999, 2007; Cruciani et al., 2005). W-directed and E- and NE-directed subductions have slab hinges respectively diverging and converging relative to the upper plate, fast versus low subduction rates (Doglioni et al., 2006, 2007), low versus high topographic envelopes (α) and high versus low foreland monoclines (β) (Doglioni et al., 2007). Finally the subducted lithospheric volume is three times bigger in W-directed subductions (Doglioni et al., 2007, 2009).

Oceanic rifts are also asymmetric, with east flanks more elevated of about 100–300 m worldwide (Doglioni et al., 2003) (Fig. 3). Moreover, along a cross section across the Mid Atlantic Ridge (MAR), Panza et al. (2010) (Fig. 3) showed that shear waves velocities (V_S) suggest a thicker western limb of the MAR and a thinner eastern limb. These authors also emphasized the occurrence of a low velocity zone (LVZ) between the lithospheric mantle (LID) and the upper asthenosphere of about 200 km depth. Using velocities of plates relative to the mantle and modelling the mantle upwelling beneath a migrating Mid Atlantic ridge, the asymmetry in the thickness and bathymetry among the two limbs at oceanic rift zones was recently reproduced by Cuffaro and Miglio (2012). Mantle depletion at the ridge was inferred to explain the smaller thermal subsidence in the eastern side of the rift zones (Panza et al., 2010). The transit of a harzburgite depleted mantle eventually moving E- or NE–ward with respect to the overlying lithosphere could explain the uplift of continental realms (e.g., Africa and Europe, Doglioni et al., 2003; Carminati et al., 2009).

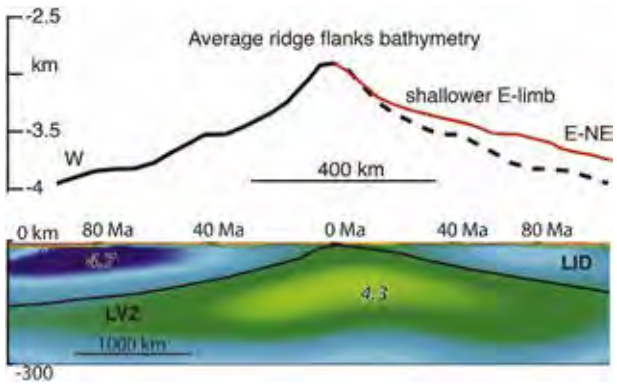

Figure 3. Upper panel – average ridge flanks bathymetry after Doglioni et al. (2003). The average depth of western flanks compiled at mid ocean ridges (black solid line) is higher with respect to the eastern one (red solid line). For a better comparison the western flank is also reported on the eastern side (black dash line) to emphasize the difference (about 100 m shallower close to the ridge and 300 m more far away in the eastern limb). Lower panel – shear waves velocities (V_S) beneath the Mid Atlantic Ridge (MAR) along the tectonic equator, after Panza et al. (2010). Data show an asymmetry between the western limb of the MAR (thicker lithosphere) and the eastern one (thinner) emphasizing a low velocity zone (LVZ) between the lithospheric mantle (LID) and the upper asthenosphere (between 100 and 200 km). Colours from light green to dark blue represent S-waves from 4.3 to 4.7 km/s, respectively.

3. Tectonically asymmetric Earth along the net rotation great circle

In this section, we present a compilation of geophysical data projected along the net rotation great circle (representing the best fit of the tectonic equator) obtained by Crespi et al. (2007) in the shallow hotspot framework. These authors have shown that the location of the net rotation pole is not markedly different if calculated assuming a deep (at latitude 53.8°S and longitude 115.7°E) or shallow (at latitude 56.4°S and longitude 136.7°E) hotspot origin (Fig. 1).

The tectonic equator of Crespi et al. (2007) crosses eight main plate tectonic features, i.e., four mid-ocean ridges (the East Pacific Rise [EPR], the Mid Atlantic [MAR], the Indian [IR], and the East African [EAR] Ridges) and four subduction zones (the Andean [AS], the Himalaya [HS], the Nankai [NS], and the Izu-Bonin [IBS] subductions) (Fig. 4a). In addition we provide plots also for small circles shifted 30° north and south of the great circle. The small circle of the net rotation pole shifted 30°N with respect to the tectonic equator crosses seven main plate tectonic features, i.e., two mid ocean ridges and one continental rift (the East Pacific Rise [EPR], the Mid Atlantic Ridge [MAR], and the Red Sea Rift [RSR]), and four subduction zones (the Aleutians [ALS], the Andean [AS], the Zagros [ZS] and the Kamchatka [KS] subductions) (Fig. 4a). Finally, the small circle of the net rotation pole shifted 30°S with respect to the tectonic equator crosses ten main plate tectonic features, i.e., three mid ocean ridges (the East Pacific Rise [EPR], the South West Indian [SWIR] and the Indian [IR] Ridges), and seven subduction zones (Tonga [TS], Antarctic Peninsula [SPS], Sandwich Subduction [SS], Indonesia [IS], Philippine [PS], Manus [MS] subductions, and Molucche subduction system [MaS], both W- and E-directed).

At these main tectonic features, and along these main plate trajectories, we explored topography, heat flow, and S-wave velocities (V_S) data. Moreover, we investigated earthquake catalogues, to study the number of events, the elastic energy release and the location of the hypocentres occurring at subduction zones. Fig. 4 shows the topography distribution worldwide after ETOPO1 model (Amante and Eakins, 2009), along the main trajectories for plate motions. ETOPO1 is a 1 arc-minute global relief model of Earth's surface that integrates land topography and ocean bathymetry and was built from numerous global and regional data sets. The cross-section diagrams (Fig. 4) show clearly that W-directed subduction zones are generally associated with accretionary prisms characterized by low-topography. Vice versa, E- and NE-directed subductions are associated with mountain belts with higher relief. This pattern can be observed on all the profiles. In addition, Fig. 4 shows the heat flow distribution worldwide after Shapiro and Ritzwoller (2004). These authors utilized the worldwide global heat flow database of Pollack et al. (1993) and used a global seismic model of the crust and upper mantle to guide the extrapolation of existing heat flow measurements to regions where

Please cite this article in press as: Doglioni, C., et al., Tectonically asymmetric Earth: From net rotation to polarized westward drift of the lithosphere, Geoscience Frontiers (2014), http://dx.doi.org/10.1016/j.gsf.2014.02.001

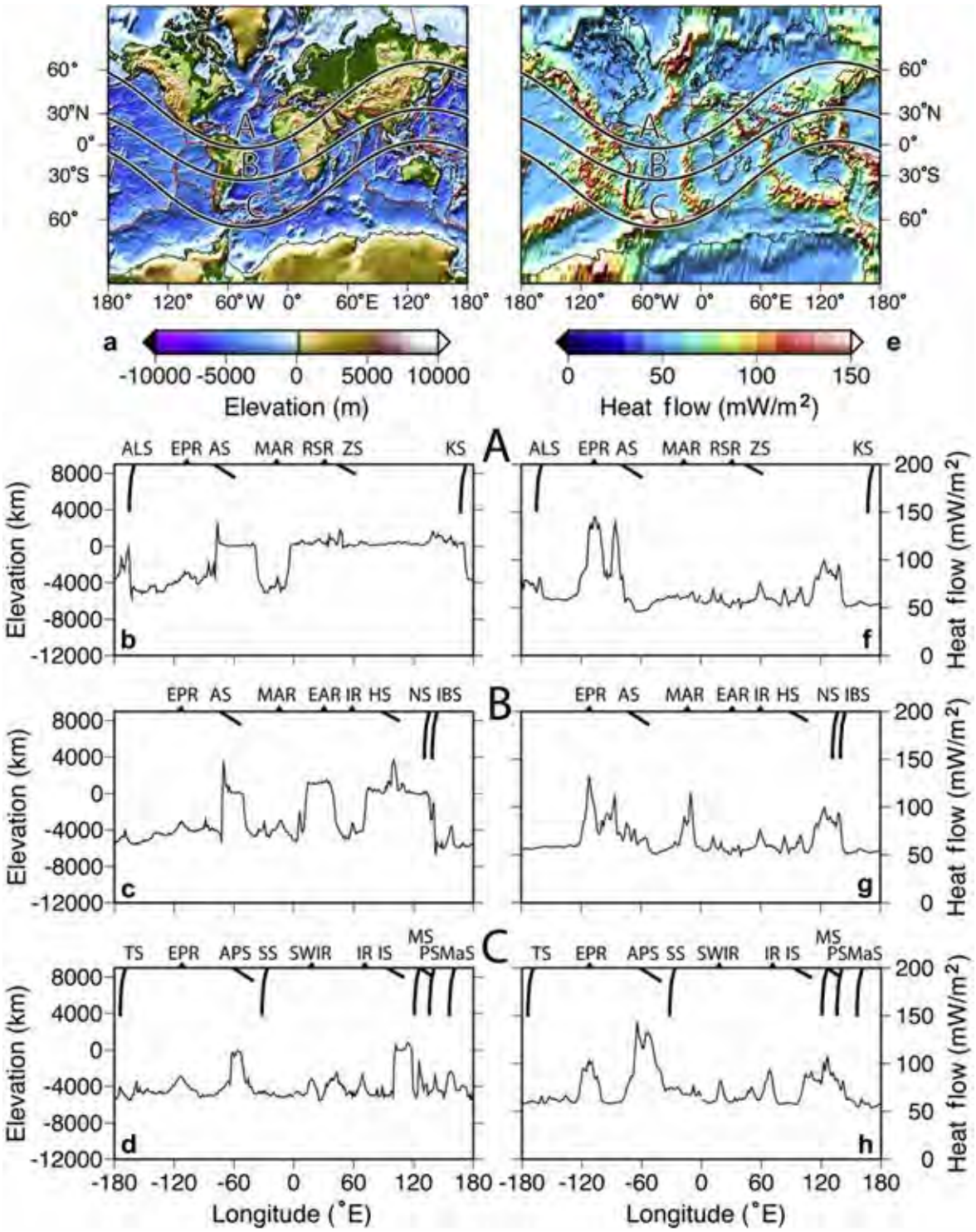

Figure 4. (a) Topography distribution worldwide after ETOPO1 model (Amante and Eakins, 2009). Lines B, A, C correspond to the tectonic equator and its related 30°N and 30°S small circles respectively. The topography cross-section diagrams (b), (c), (d), along the circles A, B, C respectively, show clearly that W-directed subduction zones are generally associated with accretionary prisms characterized by low-topography. Vice-versa, E- or NE-directed subductions are associated with mountain belts with higher relief. This pattern can be observed on all the profiles. (e) Heat flow distribution worldwide after Shapiro and Ritzwoller (2004). Apart from well known heat flow high values for mid ocean ridges and volcanic arcs, it can be observed on the heat flow cross-section diagrams (f), (g), (h), along the circles A, B, C respectively, that W-directed subduction zones are characterized by high heat flow values in backarc regions with respect to the E- or NE-directed ones. The best example is provided by the Sandwich backarc region, but high heat flow values can be observed also in the backarc of the subduction zones on the western side of the Pacific ocean. KS, Kamchatka Subduction, ALS, Aleutians Subduction, EPR, East Pacific Rise, AS, Andean Subduction, MAR, Mid Atlantic Ridge, RSR, Red Sea Rift, ZS, Subduction EAR, East African Ridge, HS, Himalaya Subduction, NS, Nankai Subduction, IBS, Izu-Bonin Subduction, TS, Tonga Subduction, APS, Antarctic Peninsula Subduction, SS, Sandwich Subduction, SWIR, South West Indian Ridge, IR, Indian Ridge, IS, Indonesia Subduction, MS, Molucche Subductions, PS, Philippine Subduction, MaS, Manus Subduction.

Please cite this article in press as: Doglioni, C., et al., Tectonically asymmetric Earth: From net rotation to polarized westward drift of the lithosphere, Geoscience Frontiers (2014), http://dx.doi.org/10.1016/j.gsf.2014.02.001

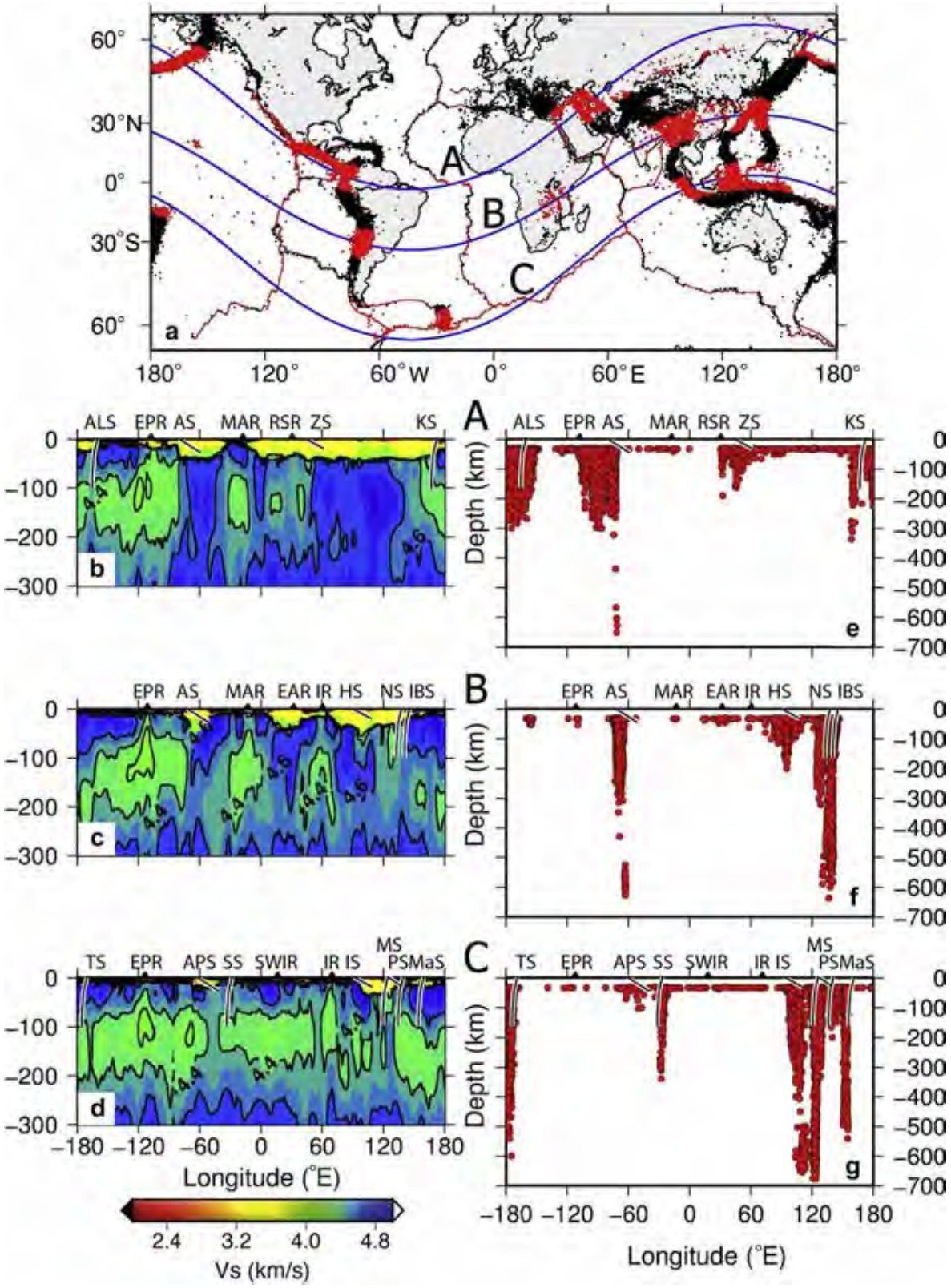

Figure 5. (a) Global seismicity from NEIC database at depth > 30 km (http://earthquake.usgs.gov/regional/neic/) with lines B, A, C corresponding to the tectonic equator and its related 30°N and 30°S small circles respectively. The cross-section diagrams (b), (c), (d), along the circles A, B, C respectively, represent the values of the shear waves velocities (V_s) after Shapiro and Ritzwoller (2002). The western limbs of rift zones have in average a deeper bathymetry with respect to the eastern ones, and that, except for section (b), an approximately continuous low velocity layer 100–200 km can be detected in the upper asthenosphere. The cross-section diagrams (e), (f), (g), along the circles A, B, C respectively, show earthquake depth and represent the red points of (a). Beneath rift zones, earthquakes occur at lower depths, whereas under subduction zones an asymmetry is detected showing continuous seismicity as far as 670 km for W-directed subductions and the presence of a deeper scattered cluster of hypocentres between 550 and 670 km for E- and NE-directed subductions. Acronyms are those of Fig. 4.

Please cite this article in press as: Doglioni, C., et al., Tectonically asymmetric Earth: From net rotation to polarized westward drift of the lithosphere, Geoscience Frontiers (2014), http://dx.doi.org/10.1016/j.gsf.2014.02.001

such measurements were rare or absent. High heat flow values are obviously visible along oceanic ridges and volcanic arcs, and in particular also along the backarc settings of W-directed subduction zones. An example is provided by the Sandwich backarc region, but high heat flow values can be observed also in the backarc of the subduction zones on the western side of the Pacific ocean.

The cross-section diagrams of Fig. 5 represent the values of shear wave velocities (V_s). We utilized the three-dimensional (3-D) shear wave velocity model of the Earth's down to 300 km, CUB2, of Shapiro and Ritzwoller (2002) (http://ciei.colorado.edu/nshapiro/MODEL/). The velocities are presented on a 2 × 2 degrees grid at the Earth's surface, and every 4 km at depth along the cross sections. In our cross-sections (Fig. 5), we plot these data interpolated applying the methods proposed by Smith et al. (1990). Fig. 3 shows that the western limbs of rift zones and mid-ocean ridges have, on average, a deeper bathymetry with respect to the eastern flanks, and an approximately continuous low velocity layer at 100–200 km depth in the upper asthenosphere. Fig. 5 also shows the depth of seismicity along the tectonic equator and its related 30°N and 30°S small circles. The seismic events, generated at depths >30 km, were extracted from the NEIC global seismicity catalogue (http://earthquake.usgs.gov/regional/neic/). The positions of the hypocentres suggest that, beneath rift zones, earthquakes occur at lower depths, whereas under subduction zones an asymmetry is detected, showing continuous seismicity as deep as 700 km in W-directed subductions, and the presence of a deeper scattered cluster of hypocentres between 550–670 km in E- and NE-directed subductions.

Figs. 6 and 7 show the depth distribution of the number of events, N, and of released energy, E, respectively. A significant amount of papers, based both on the analysis of complete (e.g., Levin and Sasorova, 2012; Riguzzi et al., 2010, and references therein), or declustered catalogues (e.g., Varga et al., 2012) analysed the depth distribution of the numbers of events, and their energy. Our diagrams are constructed using the ISC-GEM Global Instrumental Earthquake Catalogue, Version 1.01 available online at http://www.isc.ac.uk/iscgem (Bondár et al., 2012; Di Giacomo et al., 2012; Storchak et al., 2012). The Catalogue contains 16,828 seismic events that occurred from 1960 to 2009, characterized by origin date and time, epicentre, error ellipse parameters, magnitude expressed in M_w scale with an uncertainty (based on a reliable value of seismic moment or proxy M_w in all other cases) and six moment tensor components (where available). Homogeneous magnitudes allowed us to evaluate the energy dissipated by each event using the classical Gutenberg relationship (Gutenberg and Richter, 1956). The diagrams are built for the subduction zones crossed by the tectonic equators, four W-directed (1 – Philippine, 2 – Izu-Bonin, 3 – Ryukyu, 4 – Aleutians), and the other four E- or NE-directed (5 – South America, 6 – Sumatra, 7 – Himalaya and 8 – Zagros). The selected events are grouped in classes of 50 km depths.

As far as it concerns the depth vs. the number of events diagrams, we found that W-directed (Philippine, Izu–Bonin, and Ryukyu subduction zones) display continuous seismicity. Although W-directed, the Aleutians subduction is characterized by shallow seismicity. For example, South America, Sumatra and New Hebrides show, on the contrary, a seismic gap, typical of E- or NE-directed subduction zones between 300 and 550 km. Below the Himalaya and Zagros belts, associated with continental subduction zones (also termed continental collision in the literature), very shallow seismicity is observed (Fig. 6). The energy released by the selected events show for W-directed slabs, both a continuous release of energy down to 500 km with some gaps and a shallower seismic behaviour (e.g., Ryukyu and Aleutians respectively). The diagrams show the characteristic seismicity gap for E- and NE-directed slabs (South America, and Sumatra) and a well-expected shallow release of energy in the continental subduction zones (Himalaya, and Zagros) (Fig. 7).

4. From net rotation to global westward drift of the lithosphere

The above discussed data, and our interpretations point for an asymmetric Earth, and a global westward drift of the lithosphere. The hotspot reference frame is the most used system to model absolute plate motions and to estimate the westward drift of the lithosphere (e.g., Gérault et al., 2012, and reference therein). The Pacific hotspots framework is the most appropriate one, mainly because such hotspots are located in intraplate settings (Doglioni et al., 2005; Cuffaro and Doglioni, 2007).

Generally, most of the used hotspots are neither fixed, nor they represent a fixed reference frame because they are located on plate margins such as moving ridges (Galapagos, Easter Island, Iceland, Ascension, etc.), transform faults (Reunion), subduction-related volcanic arcs, or continental rifts (Afar). All these tectonic features move one relative to the others and relative to the mantle. On the contrary, the Pacific hotspots are reasonably fixed relative to each other (Norton, 2000), and their volcanic tracks can be used for the hotspot reference frame.

Thermobarometric and geochemical studies have indicated that so-called Atlantic plumes may rather be colder mantle spots, where the larger magmatism is due to the presence of fluids in the upper mantle, which decrease the melting temperature (Bonatti, 1990). Therefore the magmatic source generating the volcanic trail is located in the upper asthenosphere (e.g., Foulger et al., 2005, Foulger and Jurdy, 2007; Hirschmann, 2010; Anderson, 2011, 2013; Presnall and Gudfinnsson, 2011; and references therein). Different models to explain other "hotspots" tracks have been proposed (e.g., Foulger et al., 2005; Carminati and Doglioni, 2010). In these models, volcanoes are fed by the upper mantle or LLAMA (or Laminated Lithologies & Aligned Melt Accumulations, Anderson, 2011), and shear heating in the low-velocity layer may contribute to generate extra magmatism in the decoupling zone (Doglioni et al., 2005; Anderson, 2011). According to Moore (2008) a thermal bump occurs at the base of the boundary layer (LLAMA) and no extra heating is required. Large plate insulation also keeps the shallow mantle warm. Moreover Ritsema and Allen (2003) showed that most hotspots are anchored above 200 km.

The origin of intraplate Pacific magmatism is rather obscure, and the depth of its source and the mechanism of melting are still under discussion (e.g., Foulger et al., 2005). Doglioni et al. (2005) proposed that, if the source of the Pacific hotspots is located in the asthenosphere, especially within the upper asthenosphere or LVZ (at depth of 100–200 km), plate motions need to be faster, because the magma is supplied by the upper part of the decoupling layer separating the lithosphere from the underlying mantle. Therefore the amount of decoupling beneath the magma source is not recorded by the surficial magmatic track, which does not mark the entire shear with respect to the mantle beneath the decoupling. Cuffaro and Doglioni (2007) quantified these concepts computing plate motions relative to the deep and shallow hotspot reference frames (i.e., below the decoupling and intra-decoupling), using Pacific plate velocity, as obtained by Gripp and Gordon (2002), and incorporating the current relative plate motions NUVEL1A (DeMets et al., 1994). They found that, if the source of the Pacific hotspots is located within asthenosphere, the Pacific plate doubles its angular velocity with respect to the results obtained assuming a deep source (at depth below 400, down to 2890 km). In other words, with shallow hotspots faster global plate motions are obtained, resulting in a global westward drift of the lithosphere.

In the majority of published models, the net rotation is computed assuming a source depth below the decoupling zone between the lithosphere and the underlying mantle (e.g., Ricard et al., 1991; Gripp and Gordon, 2002), being plumes sourced

Please cite this article in press as: Doglioni, C., et al., Tectonically asymmetric Earth: From net rotation to polarized westward drift of the lithosphere, Geoscience Frontiers (2014), http://dx.doi.org/10.1016/j.gsf.2014.02.001

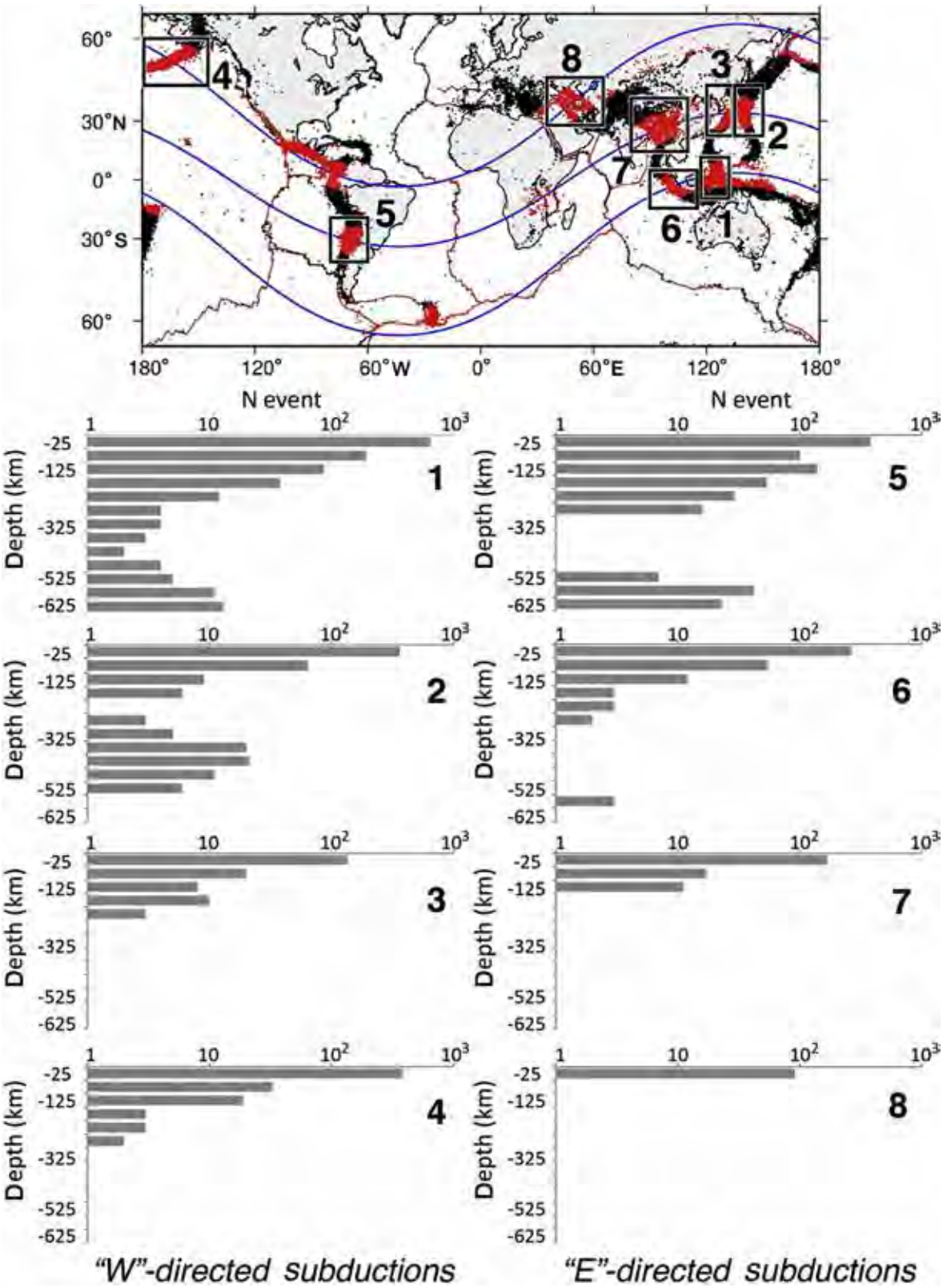

Figure 6. Global seismicity from ISC-GEM Global Instrumental Earthquake Catalogue (http://www.isc.ac.uk/iscgem), with lines corresponding to the tectonic equator and its related 30°N and 30°S small circles. These lines cross eight selected subduction zones (black rectangles), four W-directed 1 – Philippine, 2 – Izu-Bonin, 3 – Ryukyu, 4 – Aleutians, and the other four E- or NE-directed, 5 – South America, 6 – Sumatra, 7 – Himalaya and 8 – Zagros. We considered the depth distribution of the number of earthquakes, grouped in classes of 50 km depths. We found that 1, 2, and 3 have continuous number of events increasing with depth, except for 4, showing a shallow seismicity. Panels 5 and 6 show, on the contrary, the seismic gap typical of E- or NE-directed subduction zones, whereas 7 and 8, being continental subduction zones, present a very shallow seismicity.

Please cite this article in press as: Doglioni, C., et al., Tectonically asymmetric Earth: From net rotation to polarized westward drift of the lithosphere, Geoscience Frontiers (2014), http://dx.doi.org/10.1016/j.gsf.2014.02.001

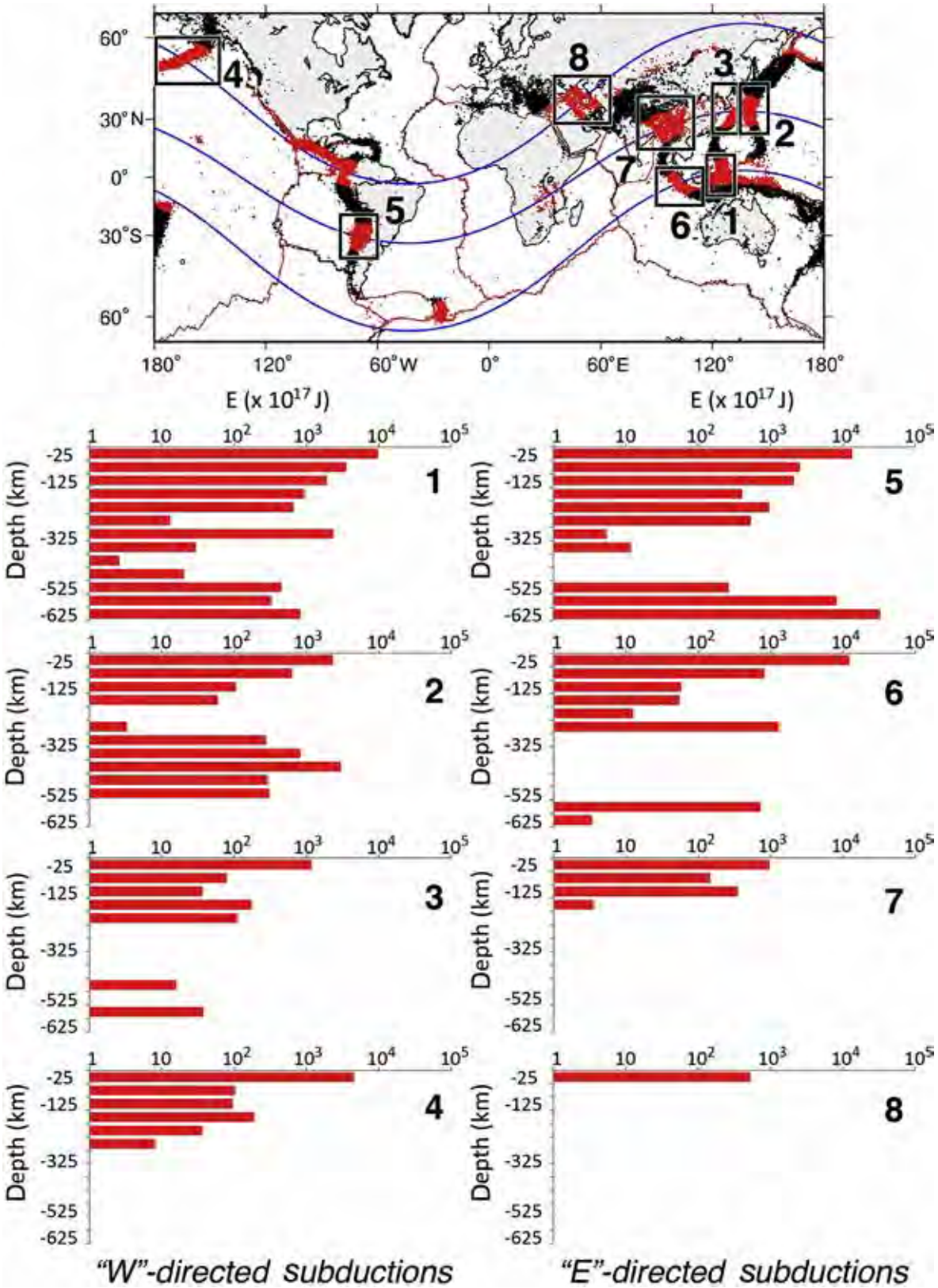

Figure 7. Global seismicity from ISC-GEM Global Instrumental Earthquake Catalogue (http://www.isc.ac.uk/iscgem), with lines corresponding to the tectonic equator and its related 330°N and 30°S small circles. These lines cross eight selected subduction zones (black rectangle), as reported in Fig. 6. We considered the elastic energy release at these zones as in Varga et al. (2012), and we found for W-directed slabs, there is a continuous release of energy till 500 km with some gap and a shallow behaviour (e.g., 3 and 4 respectively), whereas we found a the characteristic seismicity gap for E- and NE-directed slabs (5, and 6) and the well-expected shallow seismic activity for continental subduction zones (7, and 8). Both subduction zones, however, show the highest values of energy release mostly in the first 100 km.

Please cite this article in press as: Doglioni, C., et al., Tectonically asymmetric Earth: From net rotation to polarized westward drift of the lithosphere, Geoscience Frontiers (2014), http://dx.doi.org/10.1016/j.gsf.2014.02.001

directly from the core-mantle boundary. Since growing petrological and geophysical data support an asthenospheric source of the so-called plumes (e.g., Anderson, 2011; Presnall and Gudfinnsson, 2011, and references therein), to fully test the effects on kinematic models of an alternative hotspots source depth, we assume variable (intra-low velocity zone or intra-decoupling) source depths at 225, 200 and 150 km (Fig. 8). The calculations were performed following the basic assumptions proposed in Cuffaro and Doglioni (2007). Pacific hotspots indicate a decoupling between the magma source in the mantle and the oceanic lithosphere, which is moving relatively toward the WNW. If the source is below the asthenosphere (e.g., in the sub-asthenospheric mantle or deep mantle), after assuming that the shear is distributed throughout the asthenospheric channel (Gung et al., 2003), the observed seamount chain propagation rate $V_O = V_L - V_M$ represents the complete shear between the lithosphere and the mantle, here modelled as a Couette flow (Fig. 8). If the Pacific hotspots have variable source depth in the asthenosphere, a variable missing shear velocity V_x needs to be added to the observed V_O, so that the relation $V_O + V_x = V_L - V_M$ can take into account the total shear of the lithosphere with respect to the mantle (Fig. 8). Combining the Pacific plate angular velocity relative to the hotspots with the relative plate motion models proposed by DeMets et al. (1994), and applying methods used (for instance, in Gordon and Jurdy, 1986; Gripp and Gordon, 1990, 2002; Cuffaro and Jurdy, 2006; Cuffaro and Doglioni, 2007), shallow hotspots reference frames predict faster plate angular velocities ω_p and a polarized westward drift of the lithosphere. Moreover, we computed net rotation of the lithosphere relative to the mantle for each solution (i.e., at depths of 225, 200 and 150 km), referring to the plate geometrical factors I_p proposed by Argus and Gordon (1991), and using, for the total number of plates P, the relation $\omega_{NR} = \sum_{p=1}^{P} I_p \omega_p$ (Gordon and Jurdy, 1986; Jurdy, 1990; Cuffaro and Jurdy, 2006; Cuffaro and Doglioni, 2007).

In Table 1, global plate kinematic models obtained with different shallow hotspots reference frames are reported. Shallow hotspot reference frames predict faster plate motions and high value of the net rotations, i.e., 0.6451, 0.9614, and 2.5507°/Ma assuming hotspot source depths at 225, 200, and 150 km depths respectively. In Fig. 9, global plate velocities show that if the source is located at a depth of 225 km, plates move generally toward the west, except for the Nazca plate that moves slowly toward the East. On the contrary, if the source is located at depth of 200 km and 150 km respectively, plates move with higher velocities and they are strongly W-directed. Moreover, when the sources are shallower, the Euler poles for plates get closer to the net rotation pole, showing a global and polarized westward drift of the lithosphere.

Incorporating the relative motions proposed by DeMets et al. (1994) in the hotspot reference frame takes into account that the main characteristics of the tectonic features, such as directions of the orogens due to relative convergence, are maintained, when computing velocity vectors relative to the mantle. Actually, relative to the shallow hotspots, India and Eurasia plates show a parallel direction of motion along the Himalaya (Fig. 9b, c), However, the vectors of both plates are with the appropriate deviations, so that, when relative motion of India and Eurasia is computed, by making use of the Euler parameters of Table 1, the NE-ward convergence of India with respect to the fixed Eurasia can be obtained.

5. Constraints on mantle convection

The review of the global asymmetries of plate tectonic features, described in the previous sections are sketched in Fig. 10. The global and polarized westward drift of the lithosphere obtained in the shallow hotspot framework supports this asymmetric pattern. It is stressed that the fastest moving plate in both shallow and deep hotspot reference frames (i.e., the Pacific) has the lowest asthenosphere viscosity value estimated so far (the viscosity was calculated

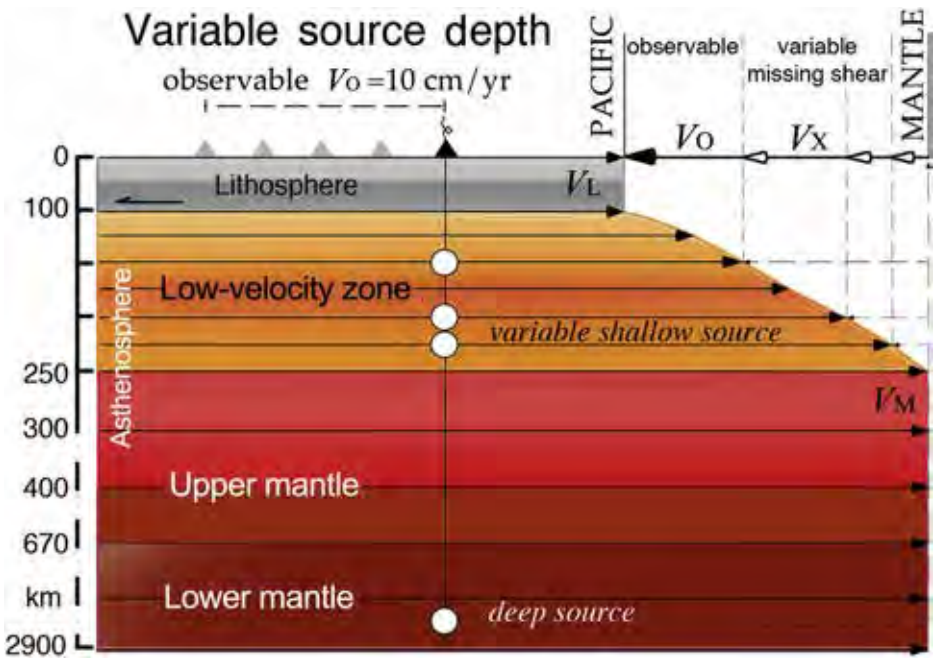

Figure 8. Pacific hotspots indicate a decoupling between the magma source in the mantle and the oceanic lithosphere, which is moving relatively toward the WNW. If the source is below the asthenosphere (e.g., in the sub-asthenospheric mantle or deep mantle), the seamount chain propagation rate $V_O = V_L - V_M$ represents the complete shear between the lithosphere and the mantle, here modelled as a Couette flow. If the Pacific hotspots have variable source depth in the asthenosphere, there is a variable missing shear velocity V_x that is needed to be added to the observed V_O, so that the relation $V_O + V_x = V_L - V_M$, can take into account the total shear of the lithosphere with respect to the mantle. This produces faster plate motions and a polarized westward drift of the lithosphere. After Doglioni et al. (2005) and Cuffaro and Doglioni (2007).

Please cite this article in press as: Doglioni, C., et al., Tectonically asymmetric Earth: From net rotation to polarized westward drift of the lithosphere, Geoscience Frontiers (2014), http://dx.doi.org/10.1016/j.gsf.2014.02.001

Table 1
Global plate motions with respect to the Pacific shallow hotspot reference frames computed incorporating the NUVELIA current plate motion model (DeMets et al., 1994), and assuming hotspots source depths $H = 225$ km, $H = 200$ km, and $H = 150$ km, respectively.

ID	$H = 225$ km			$H = 200$ km			$H = 150$ km		
	Euler pole		ω	Euler pole		ω	Euler pole		ω
	°N	°E	°Myr^{-1}	°N	°E	°Myr^{-1}	°N	°E	°Myr^{-1}
AF	−57.747	48.850	0.3819	−61.054	66.439	0.6887	−61.467	90.326	3.1839
AN	−54.825	81.228	0.4102	−57.805	84.789	0.7268	−60.345	88.458	2.3171
AR	−16.114	32.869	0.5776	−34.118	44.253	0.7845	−54.775	69.206	2.2508
AU	−12.882	49.568	0.8418	−26.412	55.625	1.0507	−48.950	71.076	2.4743
CA	−71.242	62.013	0.4827	−67.980	76.021	0.7948	−63.778	86.312	2.3804
CO	4.296	−119.555	1.0455	−12.429	−124.310	0.9357	−72.013	179.380	1.6822
EU	−61.939	82.115	0.4159	−61.795	85.705	0.7339	−61.587	88.879	2.3254
IN	−15.487	35.618	0.5939	−33.124	46.267	0.8021	−54.134	69.731	2.2667
JF	−43.377	64.824	1.2032	−47.489	68.527	1.5005	−55.166	77.851	3.0515
NA	−74.090	51.913	0.5786	−70.664	70.701	0.8861	−65.013	84.896	2.4655
NZ	1.036	−91.696	0.1605	−87.923	−124.010	0.2770	−65.823	90.757	1.8365
PA	−61.467	90.326	1.2736	−61.467	90.326	1.5919	−61.467	90.326	3.1839
PH	−59.542	−8.194	1.2980	−64.972	5.123	1.5435	−69.552	51.722	2.9853
SA	−67.673	84.485	0.6459	−65.652	86.719	0.9629	−63.054	89.089	2.5530
SC	−72.869	71.336	0.6488	−69.380	79.741	0.9613	−64.526	87.070	2.5458
NR	−58.070	75.877	0.6451	−59.363	80.320	0.9614	−60.764	86.410	2.5507

by modelling earthquake remote triggering by Pollitz et al., 1998). This suggests that the viscosity of the low-velocity zone in the upper asthenosphere can control the amount of decoupling and the velocity of the lithosphere relative to the upper mantle. Therefore, the higher the viscosity of the asthenosphere, the smaller the decoupling between the lithosphere and the asthenosphere, and the slower the velocity of the plate. Then, lateral variations in asthenosphere viscosity of the decoupling zone (LVZ) should determine velocity gradients in the overlying lithosphere, and finally control plates interactions (i.e., relative convergence or divergence; Doglioni, 1993; Cuffaro and Doglioni, 2007; Doglioni et al., 2007). Mantle circulation, associated with activity of subduction zones and mid-ocean ridges, should redistribute through time these lateral anisotropies. In particular, fluid recharge of the mantle along subduction zones should decrease the mantle viscosity and fluid extraction at mid-ocean ridges should increase it.

Therefore, the asymmetry in subduction velocity at plate boundaries should constraint models on mantle convection. In fact, subduction rates in W-directed subduction zones are three to five times faster than in E- or NE-directed slabs, providing much faster lithospheric recycling, hence a larger volume of mantle displacement, and related corner flow (Doglioni et al., 2007).

Seismic P- and S-waves tomography models show that the asthenosphere is stratified and laterally heterogeneous (e.g., Thybo, 2006; Panza et al., 2010), and its uppermost part, between 100 and 200 km of depth, defined by Anderson (2011) as the low-velocity anisotropic layer, contains a well-developed low-velocity zone, LVZ (Dziewonski and Anderson, 1981). Within the LVZ, the velocity decrease of S-waves is larger than that of P-waves, suggesting the presence of a significant amount of melt (Naif et al., 2013). This melting can be also generated by a more abundant presence of free water in the range of 100–200 km depth (Green et al., 2010).

In addition, electromagnetic studies support the presence of a thin asthenospheric layer with significant amount of fluids (Calcagnile and Panza, 1987; Adám and Panza, 1989), and melt-rich lithosphere (Naif et al., 2013) that would decrease the viscosity of the low velocity zone (LVZ). The lithosphere–asthenosphere transition (LVZ) is considered to be a zone of decoupling (e.g., Doglioni et al., 2011), being its top the Gutenberg discontinuity. In the Anderson's (2011) terminology this is part of LLAMA, or upper boundary layer, which contains the plate and lid (lithosphere), plus the LVZ. The decoupling at the base of the lithosphere can be favoured by shear heating (Doglioni et al., 2005), and calls for super-adiabatic conditions in the LVZ (Anderson, 2011). The depth and thickness of the LVZ and the related Gutenberg discontinuity varies, being deeper and thinner beneath continents. For example the LVZ top is shallower (40–75 km) beneath the Pacific plate (Schmerr, 2012) with respect to continents (200–250 km) as shown by Gung et al. (2003). Moreover, the deeper the decollement, the closer to the centre of the Earth. In fact plates containing continents move slower than oceanic plates, and this may be controlled both by the thinner development of the LVZ and by the smaller distance to the centre of rotation. Moreover, plate velocity relative to the mantle seems proportional to the viscosity of the LVZ. The fastest Pacific plate has been found to have the lowest viscosity values in its underlying LVZ (Pollitz et al., 1998).

This geodynamic model of plate motions and the polarized westward drift of the lithosphere can suggest constraints for a global model of mantle circulation. Subduction zones trigger a corner flow in the host mantle (Turcotte and Schubert, 2002). At spreading centres, diverging plates produce corner flow and passive mantle upwelling beneath mid ocean ridges (e.g., Ligi et al., 2008; Cuffaro and Miglio, 2012, and reference therein). However, the asymmetries of plate tectonics and the westward drift of the lithosphere predict that this mechanism might be valid only for W-directed subduction, whereas along the opposite settings, the mantle should be flowing upward, or sucked by the "westward" motion of the lithosphere relative to the mantle (Fig. 10) as suggested by Doglioni et al. (2009).

In this reconstruction, at a global scale the mantle would be flowing eastward relative to the lithosphere, generating a first order flow. Subduction and rift zones provide then a second order turbulence disturbing the main eastward relative mantle flow. The asthenospheric depletion at oceanic ridges makes the layer more viscous and increases the lithosphere/asthenospheric coupling, and the plate to the east is then slower. The oceanic lithosphere subducting W-ward enters the asthenosphere where it is recycled to refertilize the asthenosphere itself. Moreover, along W-directed subduction zones, slab retreat is compensated by the asthenosphere in the backarc, but it determines a downgoing corner flow in the host mantle. Conversely, along E- or NE-directed subduction zones, generally there is no space to fill in the backarc setting. However, the slab is "up going" relative to the mantle, and a suction flow from below should be produced even to the lower mantle

Please cite this article in press as: Doglioni, C., et al., Tectonically asymmetric Earth: From net rotation to polarized westward drift of the lithosphere, Geoscience Frontiers (2014), http://dx.doi.org/10.1016/j.gsf.2014.02.001

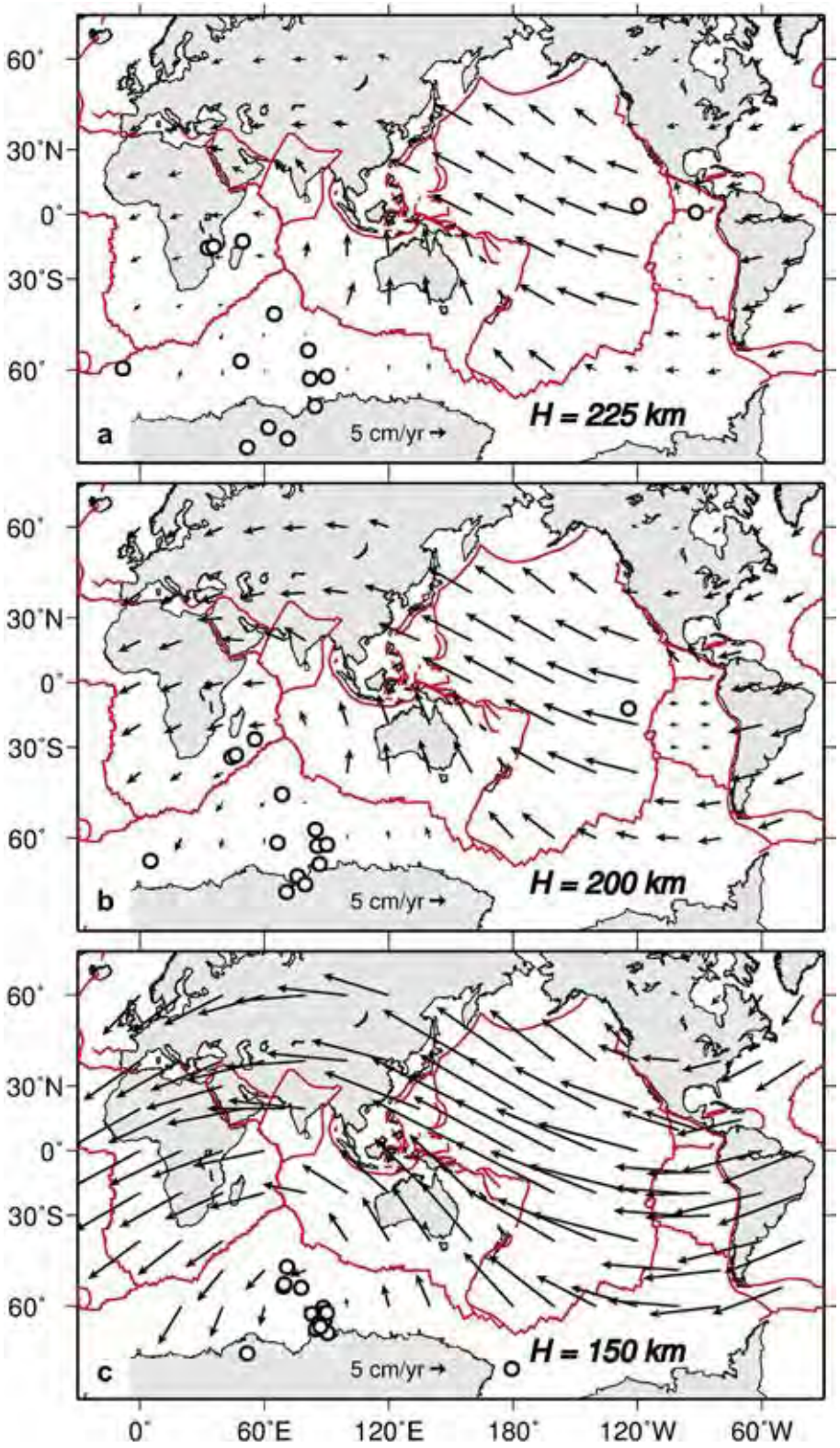

Figure 9. Present-day plate motions with respect to the Pacific shallow hotspot reference frame computed incorporating the NUVEL1A current plate motion model (DeMets et al., 1994) and assuming hotspots source depths at (a) $H = 225$ km, (b) $H = 200$ km, and (c) $H = 150$ km, respectively. Note that in (a) plates move generally toward the west, with the exception of Nazca plate that moves slowly toward the East. In (b) and (c) plates move with faster velocities and they are strongly W-directed. Open circles are the Euler poles for plates, that in (c) are located close to the net rotation pole, suggesting a global and polarized westward drift of the lithosphere.

Please cite this article in press as: Doglioni, C., et al., Tectonically asymmetric Earth: From net rotation to polarized westward drift of the lithosphere, Geoscience Frontiers (2014), http://dx.doi.org/10.1016/j.gsf.2014.02.001

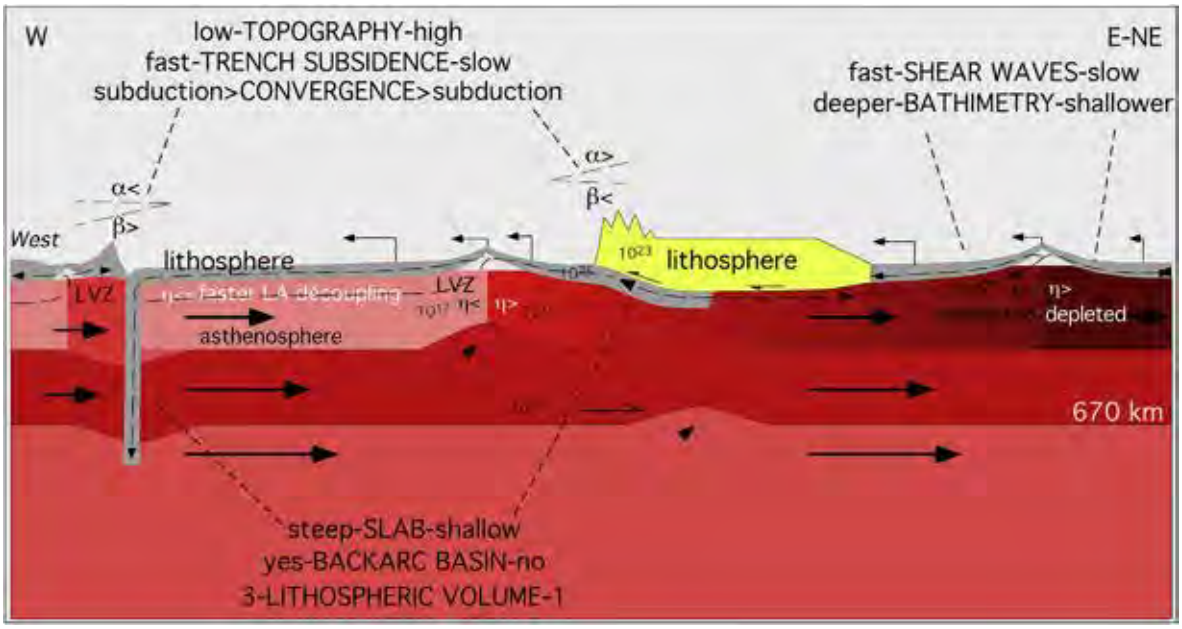

Figure 10. Summary of the global asymmetries of plate tectonic features and constraints on mantle convection, modified after Carminati and Doglioni (2012). W-directed versus E- and NE-directed subduction zones present main asymmetries such as low versus high topography, fast versus slow trench subsidence, high versus low subduction rate, low versus high topographic envelope (α), high versus low foreland monocline (β), steep versus shallow slabs, presence versus absence of backarc basins, and three versus one portions of lithospheric volume subducted, respectively. Moreover, at rift zones, the western versus eastern sides of a mid ocean ridge have fast versus slow S-wave velocities and deep versus shallow bathymetry, respectively. All these asymmetries for plate tectonics suggest a polarized westward drift of the lithosphere. Faster plate velocities may correspond to lower viscosity. The asthenospheric depletion at oceanic ridges makes the layer more viscous and increases the lithosphere/asthenospheric coupling, and the plate to the east is then slower. The oceanic lithosphere subducting E-ward enters the asthenosphere where it is molten again to refertilize the asthenosphere itself. W-directed subductions provide deeper circulation. The subduction zones disturb or deviate the general eastward flow of the mantle relative to the lithosphere. W-directed slabs produce a corner flow, whereas the opposite slab should rather generate an upward suction flow from the underlying mantle, being the cause for deep seismicity and the gap observed in the earthquake catalogues for the E- and NE-directed subduction zones.

(Fig. 10), being the cause for deep seismicity and the gap observed in the earthquake catalogues for the E- and NE-directed subduction zones (Riguzzi et al., 2010). In fact, relative to the sub-lithospheric mantle, the lower plate is moving westward out of the mantle, in the direction opposed to the dip of the slab. In these cases, the subduction process can exist because the upper plate is moving westward faster than the lower plate (Doglioni et al., 2007).

The fluids released from the slab into the overlying mantle should trigger a decrease of viscosity in the hanging wall of the subduction, at the bottom of the upper plate. The decrease of the viscosity should accelerate the relative decoupling (Doglioni et al., 2009). Therefore the upper plate increases its velocity moving away from the lower plate along the W-directed subduction zones. This facilitates backarc spreading (Fig. 10). Conversely, along the E- or NE-directed subduction zones, the upper plate is converging faster with respect to the lower plate, facilitating the generation of double verging orogens such as the Andes or Himalaya.

6. Discussion and conclusions

The literature on plate motions does not recognize the possibility of a net drift of the outer shell over the mantle. Various relative and “mantle” reference frames (both NNR and NR) movements (e.g., O’Connell et al., 1991; Gripp and Gordon, 2002; Torsvik et al., 2010; Argus et al., 2011) are used, all of which are arbitrary and chosen for convenience. Most of the data used would still be satisfied if a uniform westward drift were superposed on the “mantle reference” motions determined.

This study supports the view that (1) plate motions are not randomly distributed (Doglioni, 1990; Crespi et al., 2007); (2) plate motions have a tectonic equator that closely overlaps the equator of the net rotation of the lithosphere relative to the mantle; (3) asymmetries of plate tectonics features, show a global pattern, implying an eastward motion of the mantle relative to the lithosphere, and vice-versa, regardless the choice of the reference frame; (4) only a net rotation of the lithosphere $>1°$/Ma can account for the tectonic asymmetries observed at plate boundaries. The observed asymmetries are most consistent with so-called hotspot tracks if the magma source is located near 150–200 km, that is, in or just below the surface boundary layer and the decoupling zone. In the following Appendix A, some characteristics of the asymmetric Earth are discussed, being features that can be explained by our geodynamic model.

In conclusion, the tectonically asymmetric Earth suggests a global polarized motion of the lithosphere. This is confirmed by geological and geophysical data (i.e., the asymmetries), and by plate kinematic models relative to the Pacific shallow reference frame. Westward drift can constraint mantle circulations, and several lines of evidence suggest that sufficiently low values of viscosity can exist in the asthenosphere and in the low velocity zone. Future geodynamic models should take into account these constraints as initial and boundary conditions, so that results may be used to validate plate dynamic models of tidal drag applied on the whole lithosphere.

Acknowledgements

Discussions with, E. Bonatti, G. Panza and F. Innocenti were very stimulating. Comments by D. Anderson and E. Garzanti were extremely useful to improve the paper. Many of the figures were made with the Generic Mapping Tools of Wessel and Smith (1995). Research supported by Sapienza University of Rome and Miur-Prin 2011.

Please cite this article in press as: Doglioni, C., et al., Tectonically asymmetric Earth: From net rotation to polarized westward drift of the lithosphere, Geoscience Frontiers (2014), http://dx.doi.org/10.1016/j.gsf.2014.02.001

Appendix A

A.1. Plate motions and source depth of hotspots

In this paper, we have investigated the shallow hotspots reference frame and we have presented variable solutions for plate motions considering different depths for the hotspot source (225, 200, and 150 km) in the low velocity zone. Our main result is that at source depth of 200 km, the westward drift of the lithosphere is globally observed. Here, we used the NUVEL1A (DeMets et al., 1994), instead of recent relative plate kinematic model MORVEL (DeMets et al., 2010), to integrate our results with those obtained by Cuffaro and Doglioni (2007), who investigated the deep hotspots frame (source depth at 400 km and below) and the shallow one (source depth at 250 km in the middle of the asthenosphere) with similar data (i.e., NUVEL1A).

The choice of the Pacific hotspot frame generates higher net rotations of the lithosphere, because no tracks of African hotspots are taken into account. A slower result was obtained for current plate motions by Torsvik et al. (2010) both using Pacific and African hotspots. Also Zheng et al. (2010), using recomputed Pacific hotspots rate and incorporating recent current plate motion models (e.g., MORVEL, DeMets et al., 2010), obtained a 23% slower velocity of the Pacific plate with respect to that obtained by Gripp and Gordon (2002). These comments represent an invariant for the definition of the shallow hotspot reference frame. Assuming a source of the hotspots in the upper asthenosphere (LVZ or base LLAMA) generate faster plate motions and a global and polarized westward drift of the lithosphere, independently of the choice of the number of hotspot tracks. Moreover, plate motions presented in this paper, are independent of the existence of the tectonic equator and global mainstream of plate motions, as obtained by Crespi et al. (2007), because are computed without any constraints on directions of tectonic features. The obtained results (Fig. 9) are in agreement with the geodynamic models of rift and subduction zones, and here we found the lower limit for the depth of the hotspots, where a polarized motions of the lithosphere become quantitatively evident (e.g., 200 km).

A.2. Subduction polarity and volcanism

The different kinematics of the slabs at W- and E- or NE-directed subduction zones point to different volumes of subducted mantle (on average three times larger in the W-directed subductions, (Doglioni et al., 2007, 2009). The larger volumes subducted along W-directed slabs favour the formation of a greater amount of arc-related magma, because the athenospheric mantle wedge is thicker and hotter and should have a thicker column of potential melting (Fig. 10). Along the E-dipping subductions, the mantle wedge, hydrated by slab-delivered fluids, is mostly lithospheric in nature and cooler. The subduction rate is also smaller, and andesites are generally dominant (Doglioni et al., 2009).

Moreover, this larger recycling the related mantle convection should be 1–3 times larger along W-directed subduction zones with respect to the opposite slabs (Doglioni et al., 2007). This enhances slab-induced corner flow in the mantle in W-directed subduction zones, whereas an upward suction of the mantle is predicted along the E- or NNE-directed slabs, which provides a mechanism for syn-subduction alkaline magmatism in the upper plate, with or without contemporaneous rifting in the backarc.

Doglioni et al. (2007) showed that also metallogenesis, known to be controlled by subduction style (Mitchell and Garson, 1981), is different in the two end member subductions. W-directed subductions are characterized by Kuroko or similar volcanogenic sulfide deposits (Nishiwaki and Uyeda, 1983), whereas porphyry copper deposits (John et al., 2010) are instead located in collisional settings and E-directed (Andean-type) subduction zones.

A.3. Subduction polarity and slab geometry

Asymmetries in the slab inclinations suggest a net rotation of the lithosphere (Bostrom, 1971; Uyeda and Kanamori, 1979; Doglioni, 1990). Lallemand et al. (2005) found only a small difference between the average dip of W- versus E-directed slab. However, in order to test the Lallemand et al. (2005) results, Riguzzi et al. (2010) recomputed the slab dip, using earthquake hypocentres at subduction zones worldwide. In general, the W-directed subduction zones dip, on average, $(65 \pm 15)^\circ$, whereas the mean dip of the E- or NE-directed slabs is $(27 \pm 14)^\circ$ (Fig. 2). In addition, the steeper W-directed slabs (Uyeda and Kanamori, 1979) extend to greater depths and they present a more coherent slab-related seismicity from the surface down to the 670 km discontinuity, showing remarkable differences (Riguzzi et al., 2010). On the contrary, E- or NE-directed slab are in general, shorter than the W-directed ones and they are characterized by a seismic gap, around 300–550 km (Fig. 2), as also verified by Varga et al. (2012), and by this study, along main trajectories for plate motions (Figs. 6 and 7). These results are significantly different from those of Lallemand et al. (2005), and the main reason could be the arbitrary connection of the shallow slab seismicity with the deep isolated clusters along the E- or NE-directed subduction zones, as proposed by Riguzzi et al. (2010). In fact, high-velocity bodies, suggesting the presence of slabs in tomographic images, often present a misfit compared with slab seismicity, and the velocity model dependence of these images can produce misleading interpretations, when inferring the presence of slab deeper than 250 km (Anderson, 2006; Agostini et al., 2010; Foulger et al., 2013). It is also quite common claiming whole mantle convection, deep slab penetration or whole mantle plumes to connect isolated patches of low or high wave-speed and infer continuity. However chemical heterogeneity (e.g., Fe content variation) may induce misleading interpretations (Trampert et al., 2004).

Several studies explained slab dip angles without any use of the net rotation of the lithosphere. For example, Hager and O'Connell (1978) used plate motion relative to the no-net-rotation (NNR) reference frame, and Faccenna et al. (2007) found that slab dip angles can be controlled by regional mantle dynamics and plate properties. The no-net-rotation (NNR) framework is a conventional framework based on the assumption that no net torque can be exerted by the lithosphere on the asthenosphere (Solomon and Sleep, 1974). This approach does not yield a unique solution for absolute motions, because the nature and lateral variation of the coupling between the lithosphere and the asthenosphere are still, in a large part, unknown. The simplest no-net-rotation (NNR) condition, in which the summatory of the decoupling between the lithosphere and asthenosphere is assumed to be zero is not acceptable for the constraints derived from the mantle reference frames and for the asymmetries that can be observed at plate boundaries and in the LVZ itself. Although the possibility that local mantle dynamics can control slab dip angles (Faccenna et al., 2007) is self-consistent, the global asymmetries of plate tectonic feature strongly suggest a polarized westward drift, and a global dynamic control of the forces acting on the lithosphere.

A.4. Subduction kinematics, seismicity and state of stress

As largely discussed, seismicity is deeper in W-directed subduction zones (often reaching the 670 km discontinuity), whereas it is shallower in E–ENE directed subductions. In these latter, where deep seismicity is observed, it is associated with the occurrence of a

Please cite this article in press as: Doglioni, C., et al., Tectonically asymmetric Earth: From net rotation to polarized westward drift of the lithosphere, Geoscience Frontiers (2014), http://dx.doi.org/10.1016/j.gsf.2014.02.001

seismicity gap at intermediate depths (300–450 km). The energy released by seismicity follows the same trends in the two end-member subductions (Fig. 6).

The causes can be found in the different kinematics of the two subductions. It has been shown that subduction rates are on average three times larger in W-directed subductions. This implies that the recovery of the thermal anomaly of the subducting slab (with respect to ambient mantle) will be more effective in E–ENE directed subductions. This inference, coupled with the observation that E–ENE directed subductions are shallower than W-directed subductions, suggests that, at a given depth, E–ENE directed slabs are warmer than W-directed slabs. Metastable olivine wedges are expected to occur in slabs characterized by fast subduction of old lithosphere (e.g., Bina, 1996, 1997). The sudden transition of olivine to spinel in metastable olivine wedges was suggested to be the cause of deep earthquakes in subduction zones (e.g., Green et al., 1990; Green and Zhou, 1996). The kinematics of subduction zones presented in this work is compatible with this model of earthquake generation, since olivine wedges are expected to occur in the cold and fast W-directed subduction and to be absent in the E–ENE directed subductions.

Another view attributes the occurrence of deep earthquakes to the occurrence and reactivation in a brittle regime of preserved zones of weakness (Silver et al., 1995). The main criticism moved to this hypothesis was that, at the bottom of the upper mantle, pressure would be so high (frictional strengths increase with depth) that the shear stresses necessary to produce brittle faulting at several hundred kilometres depth were considered too high (e.g., Jeffreys, 1929). Owing to the increase of temperature, deformation at those depths would be more likely to occur with plastic mechanisms (ductile deformation rather than failure). Carminati et al. (2002, 2005) showed that brittle behaviour persists at deep upper mantle depths in slabs characterized by fast subduction rates. W-directed slabs, being steep and subducting fast are the best candidates to maintain brittle behaviour at depth. This explains why seismicity is continuous in these realms.

The disappearance of seismicity in several E–ENE directed subduction zones is here interpreted as the result of the thermal recovery (and associated reworking in the mantle) of the shallow and slowly subducting slabs. Thus, such slabs should not reach the deep upper mantle or, eventually, they should reach it strongly deformed, partly recovered by the mantle and deforming ductilely. However, in the literature the deep earthquakes occurring in E–ENE directed subduction zones have been linked with shallow seismicity (e.g., Silver et al., 1995; Omori et al., 2004) to generate continuous subducting slabs from shallow to deep upper mantle depths. The absence of seismicity at intermediate depths in some subduction zones has been in these models explained as due to uneffective dehydration embrittlement (e.g., Omori et al., 2004). Riguzzi et al. (2010) proposed an alternative view. As discussed earlier, the slab moves upward relative to the mantle in E–ENE directed subductions. The generated suction flow from below should be propagate down to the lower mantle (Fig. 10). This could explain the deep seismicity (in the Riguzzi's et al., (2010) view unrelated to the occurrence of a slab) and the gap observed in the earthquake catalogues for the E- and NE-directed subduction zones.

Also the state of stress of slabs is controlled by absolute plate motion. As discussed and shown in a recent review (Doglioni et al., 2007), stress data show that down–dip extension dominates, at intermediate depths, in E- or NE-directed slabs (e.g., the Nazca plate in the Chile subduction zone, Isacks and Molnar (1971); Rietbrock and Waldhauser (2004) and the Cocos plate in the Mexican subduction zone, Manea et al., (2006) and downdip compression occurs in west directed slabs (e.g., Tonga; Chen and Brudzinski, 2001; Chen et al., 2004). Downdip compression is typical in deep earthquakes in slabs at the 670 km transition, consistent with our observations that W-directed slabs are steep and fast, and thus can easily reach the upper–lower mantle boundary (Isacks and Molnar, 1971). It has been suggested that, in these cases, down-dip compression may be related to the viscosity increase occurring at the 670 km transition and to the thermo-dynamic effects of the phase change at this horizon (Isacks and Molnar, 1971; Vassiliou and Hager, 1988). These two processes should increase the resistance encountered by the subducting slab and be associated with compression.

The occurrence of downdip compression at intermediate depths in slabs not reaching the 670 km discontinuity is, however, enigmatic, since slab pull should put the slab into tension (e.g., Anderson, 2001; Conrad and Lithgow-Bertelloni, 2002). The origin of compression at intermediate depths has been investigated by Bina (1996, 1997), who suggested that the occurrence of metastable olivine wedges in a fast subducting oceanic lithosphere could create positive density anomalies that could partly counteract the effects of slab pull, and account for downdip compression. Although this interpretation is consistent with the fact that metastable olivine wedges are expected in the faster and steeper W-directed subductions (where downdip compression is normally observed, an alternative explanation is here preferred. As proposed by Doglioni et al. (2007) and verified with numerical models by Carminati and Petricca (2010), the state of stress in slabs is likely to be controlled by absolute plate motions. In particular, down-dip compression in the subducting slab is enhanced by mantle flow opposing the direction of the dip of the slab, whereas down-dip extension is favoured by mantle flow in the same direction of the slab dip (i.e., sustaining it).

A.5. Origin of the westward drift

All these data and interpretations point for an asymmetric Earth, whose nature is here tentatively related to the Earths rotation and its tidal despinning (Riguzzi et al., 2010). Tidal drag maintains the lithosphere under a permanent high frequency vibration, polarized and sheared toward the west (Doglioni et al., 2011). Earths rotation and the resisting force exerted by the lag of the tidal bulge (Le Pichon, 1968; Bostrom, 1971; Knopoff and Leeds, 1972; Moore, 1973; Scoppola et al., 2006) were proved to be efficient only if very low viscosity material occurs at the lithosphere asthenosphere transition. Jordan (1974), Ricard et al. (1991) and Ranalli (2000) have demonstrated that this hypothesis is incompatible with current estimates of upper mantle viscosities. It is clear that a main and crucial key point is to determine realistic values for the viscosity of the asthenosphere. Post-glacial rebound analysis provided important constraints on mantle viscosity structure, but the use of this method cannot reveal a relatively thin low viscosity layer hosted in the asthenospheric low-velocity mantle (Scoppola et al., 2006; Doglioni et al., 2011, and reference therein). Moreover, the viscosity in the asthenospheric low velocity zone can be even three orders of magnitude lower when measured under horizontal shear with respect to the viscosity computed by vertical unloading due to post-glacial rebound (Scoppola et al., 2006; Riguzzi et al., 2010; Doglioni et al., 2011). This is confirmed by Jin et al. (1994) who showed how intra-crystalline melt in the asthenospheric peridotites under shear could generate a viscosity as low 10^{12} Pa s, compatible with the efficiency of tidal drag. These very low values require the presence of high melt fractions, which is compatible with a hotter than expected asthenosphere (Anderson, 2011) and the low values of radial anisotropy in the low-velocity zone (Panza et al., 2010). Anderson (2013) inferred that temperatures at 200 km

Please cite this article in press as: Doglioni, C., et al., Tectonically asymmetric Earth: From net rotation to polarized westward drift of the lithosphere, Geoscience Frontiers (2014), http://dx.doi.org/10.1016/j.gsf.2014.02.001

can be up to ~1600 °C, which explains the low strength/viscosity as well as temperatures of some midplate magmas (Hawaii).

References

Adám, A., Panza, G.F., 1989. A critical review of the magnetotelluric information on the upper mantle. Acta Geod. Geoph. Mont. Hung. 24, 395–415.
Agostini, S., Doglioni, C., Innocenti, F., Manetti, P., Tonarini, S., 2010. On the geodynamics of the Aegean rift. Tectonophysics 488, 7–21.
Alpert, L., Becker, T.W., Bailey, I.W., 2010. Global slab deformation and centroid moment constraints on viscosity. Geochemistry, Geophysics, Geosystems 11. http://dx.doi.org/10.1029/2010GC003301.
Amante, C., Eakins, B.W., 2009. ETOPO1 1 Arc-Minute Global Relief Model: Procedures, Data Sources and Analysis. In: NOAA Technical Memorandum. NESDIS NGDC-24, 19 pp.
Anderson, D.L., 2001. Topside tectonics. Science 293, 2016–2018.
Anderson, D.L., 2006. Speculations on the nature and cause of mantle heterogeneity. Tectonophysics 416, 7–22.
Anderson, D.L., 2011. Hawaii, boundary layers and ambient mantle geophysical constraints. Journal of Petrology 52, 1547–1577.
Anderson, D.L., 2013. The persistent mantle plume myth. Australian Journal of Earth Sciences 60, 657–673. http://dx.doi.org/10.1080/08120099.2013.835283.
Argus, D.F., Gordon, R.G., 1991. No-net-rotation model of current plate velocities incorporating plate motion model NUVEL-1. Geophysical Research Letters 18, 2039–2042.
Argus, D.F., Gordon, R.G., DeMets, C., 2011. Geologically current motion of 56 plates relative to the no-net-rotation reference frame. Geochemistry, Geophysics, Geosystems 12, 11. http://dx.doi.org/10.1029/2011GC003751.
Becker, T.W., 2006. On the effect of temperature and strain-rate dependent viscosity on global mantle flow, net rotation, and plate-driving forces. Geophysical Journal International 167, 943–957.
Bina, C.R., 1996. Phase transition buoyancy contributions to stresses in subducting lithosphere. Geophysical Research Letters 23. http://dx.doi.org/10.1029/96GL03483.
Bina, C.R., 1997. Patterns of deep seismicity reflect buoy-ancy stresses due to phase transitions. Geophysical Research Letters 24, 3301–3304.
Bonatti, E., 1990. Not so hot "hot spots" in the oceanic mantle. Science 250, 107–110.
Bondár, I., Engdahl, E.R., Villasenor, A., Storchak, D., 2012. ISC-GEM: Global Instrumental Earthquake Catalogue (1900–2009): I. Location and seismicity patterns. In: AGU Fall Meeting. San-Francisco, USA.
Bostrom, R.C., 1971. Westward displacement of the lithosphere. Nature 234, 536–538.
Calcagnile, G., Panza, G.F., 1987. Properties of the lithosphere–asthenosphere system in Europe with a view toward earth conductivity. Pure and Applied Geophysics 125, 241–254.
Carminati, E., Cuffaro, M., Doglioni, C., 2009. Cenozoic uplift of Europe. Tectonics 28, TC4016. http://dx.doi.org/10.1029/2009TC002472.
Carminati, E., Doglioni, C., 2010. North Atlantic geoid high, volcanism and glaciations. Geophysical Research Letters 37.
Carminati, E., Doglioni, C., 2012. Alps vs. Apennines: the paradigm of a tectonically asymmetric Earth. Earth-Science Reviews 112, 67–96.
Carminati, E., Doglioni, C., Scrocca, D., 2005. Magnitude and causes of long-term subsidence of the Po Plain and Venetian region. In: Fletcher, C.A., Spencer, T., Mosto, J.D., Campostrini, P. (Eds.), Flooding and Environmental Challenges for Venice and its Lagoon: State of Knowledge. Cambridge University Press.
Carminati, E., Giardina, F., Doglioni, C., 2002. Rheological control of subcrustal seismicity in the Apennines subduction (Italy). Geophysical Research Letters 29. http://dx.doi.org/10.1029/2001GL014084.
Carminati, E., Petricca, P., 2010. State of stress in slabs as a function of large scale plate kinematics. Geochemistry, Geophysics, Geosystems 11. http://dx.doi.org/10.1029/2009GC003003.
Chen, E.P., Brudzinski, M.R., 2001. Evidence for a large–scale remnant of subducted lithosphere beneath Fiji. Science 292, 2475–2479.
Chen, P.F., Bina, C.R., Okal, E.A., 2004. A global survey of stress orientations in subducting slabs as revealed by intermediate depth earthquakes. Geophysical Journal International 159, 721–733.
Conrad, C.P., Behn, M., 2010. Constraints on lithosphere net rotation and asthenospheric viscosity from global mantle flow models and seismic anisotropy. Geochemistry, Geophysics, Geosystems 11. http://dx.doi.org/10.1029/2009GC002970.
Conrad, C.P., Lithgow-Bertelloni, C., 2002. How mantle slabs drive plate tectonics. Science 298, 207–209.
Crespi, M., Cuffaro, M., Doglioni, C., Giannone, F., Riguzzi, F., 2007. Space geodesy validation of the global lithospheric flow. Geophysical Journal International 168, 491–506.
Cruciani, C., Carminati, E., Doglioni, C., 2005. Slab dip vs. lithosphere age: no direct function. Earth and Planetary Science Letters 238, 298–310.
Cuffaro, M., Caputo, M., Doglioni, C., 2008. Plate sub-rotations. Tectonics 27, TC4007. http://dx.doi.org/10.1029/2007TC002182.
Cuffaro, M., Doglioni, C., 2007. Global kinematics in deep versus shallow hotspot reference frames. In: Foulger, G.R., Jurdy, D.M. (Eds.), The Origins of Melting Anomalies: Plumes, Plates, and Planetary Processes, Geol. Soc. Am. Sp. Paper, vol. 430, pp. 359–374.
Cuffaro, M., Jurdy, D.M., 2006. Microplate motions in the hotspot reference frame. Terra Nova 18, 276–281.
Cuffaro, M., Miglio, E., 2012. Asymmetry of thermal structure at slow-spreading ridges: geodynamics and numerical modeling. Computers & Fluids 68, 29–37.
DeMets, C., Gordon, R.G., Argus, D.F., 2010. Geologically current plate motions. Geophysical Journal International 181, 1–80.
DeMets, C., Gordon, R.G., Argus, D.F., Stein, S., 1994. Effect of recent revisions to the geomagnetic reversal time scale on estimates of current plate motions. Geophysical Research Letters 21, 2121–2194.
Dickinson, W.R., 1978. Plate tectonic evolution of North Pacific rim. Journal of Physics of the Earth 26 (Suppl.), S1–S19.
Di Giacomo, D., Bondár, I., Lee, W.H.K., Engdahl, E.R., Bormann, P., Storchak, D., 2012. ISC-GEM: Global Instrumental Earthquake Catalogue (1900-2009): II. Earthquake magnitudes. In: AGU Fall Meeting. San-Francisco, USA.
Doglioni, C., 1990. The global tectonic pattern. Journal of Geodynamics 12, 21–38.
Doglioni, C., 1993. Geological evidence for a global tectonic polarity. Journal of the Geological Society London 150, 991–1002.
Doglioni, C., Carminati, E., Bonatti, E., 2003. Rift asymmetry and continental uplift. Tectonics 22.
Doglioni, C., Carminati, E., Cuffaro, M., 2006. Simple kinematics of subduction zones. International Geology Review 48, 479–493.
Doglioni, C., Carminati, E., Cuffaro, M., Scrocca, D., 2007. Subduction kinematics and dynamic constraints. Earth-Science Reviews 83, 125–175.
Doglioni, C., Green, D., Mongelli, F., 2005. On the shallow origin of hotspots and the westward drift of the lithosphere. In: Foulger, G.R., Natland, J.H., Presnall, D.C., Anderson, D.L. (Eds.), Plates, Plumes and Paradigms, Geol. Soc. Am. Spec. Publ., pp. 735–749.
Doglioni, C., Harabaglia, P., Merlini, S., Mongelli, F., Peccerillo, A., Piromallo, C., 1999. Orogens and slabs vs their direction of subduction. Earth-Science Reviews 45, 167–208.
Doglioni, C., Ismail-Zadeh, A., Panza, G.F., Riguzzi, F., 2011. Lithosphere-asthenosphere viscosity contrast and decoupling. Physics of the Earth and Planetary Interiors 189, 1–8.
Doglioni, C., Tonarini, S., Innocenti, F., 2009. Mantle wedge asymmetries and geochemical signatures along W- and E-NE-directed subduction zones. Lithos 113, 179–189.
Doubrovine, P.V., Steinberger, B., Torsvik, T.H., 2012. Absolute plate motions in a reference frame defined by moving hotspots in the Pacific, Atlantic and Indian oceans. Journal of Geophysical Research 117, B09101. http://dx.doi.org/10.1029/2011JB009072.
Dziewonski, A.M., Anderson, D.L., 1981. Preliminary reference Earth model. Physics of the Earth and Planetary Interiors 25, 297–356.
Faccenna, C., Heuret, A., Funiciello, F., Lallemand, S., Becker, T.W., 2007. Predicting trench and plate motion from the dynamics of a strong slab. Earth and Planetary Science Letters 257, 29–36.
Foulger, G.R., Jurdy, D.M., 2007. The Origins of Melting Anomalies: Plumes, Plates, and Planetary Processes. In: Geol. Soc. Am. Sp. Paper. 430. http://dx.doi.org/10.1130/2007.2430(01).
Foulger, G.R., Natland, J.H., Presnall, D.C., Anderson, D.L., 2005. Plates, Plumes, and Paradigms. In: GSA Sp. Paper 388.
Foulger, G.R., Panza, G.F., Artemieva, I.M., Bastow, I.D., Cammarano, F., Evans, J.R., Hamilton, W.B., Julian, B.R., Lustrino, M., znd, T.B., Yanovskaya, H.T., 2013. Caveats on tomographic images. Terra Nova 25, 259–281.
Garzanti, E., Doglioni, C., Vezzoli, G., Andò, S., 2007. Orogenic belts and orogenic sediment provenances. The Journal of Geology 115, 315–334.
Gérault, M., Becker, T.W., Kaus, B.J.P., Faccenna, C., Moresi, L., Husson, L., 2012. The role of slabs and oceanic plate geometry in the net rotation of the lithosphere, trench motions, and slab return flow. Geochemistry, Geophysics, Geosystems 13. http://dx.doi.org/10.1029/2011GC003934.
Gordon, R.G., Jurdy, D.M., 1986. Cenozoic global plate motions. Journal of Geophysical Research 91, 12384–12406.
Green, D.H., Hibberson, W.O., Kovacs, I., Kovacs, A., 2010. Water and its influence on the lithosphere–asthenosphere boundary. Nature 467, 448–451.
Green, H.W., Young, T.E., Walker, D., Scholz, C.H., 1990. Anticrack–associated faulting at very high pressure in natural olivine. Nature 348, 720–722.
Green, H.W., Zhou, Y., 1996. Transformation–induced faulting requires an exothermic reaction and explains the cessation of earthquakes at the base of the mantle transition zone. Tectonophysics 256, 39–56.
Gripp, A.E., Gordon, R.G., 1990. Current plate velocities relative to the hotspots incorporating NUVEL-1 global plate motion. Geophysical Research Letters 17, 1109–1112.
Gripp, A.E., Gordon, R.G., 2002. Young tracks of hotspots and current plate velocities. Geophysical Journal International 150, 321–364.
Gung, Y., Panning, M., Romanowicz, B., 2003. Global anisotropy and the thickness of continents. Nature 422, 707–711.
Gutenberg, B., Richter, C.F., 1956. Earthquake magnitude, intensity, energy and acceleration (second paper). Bull. Seism. Soc. Am. 46, 105–145.
Hager, B.H., O'Connell, R.J., 1978. Subduction zone dip angles and flow derived by plate motion. Tectonophysics 50, 111–133.
Harabaglia, P., Doglioni, C., 1998. Topography and gravity across subduction zones. Geophysical Research Letters 25, 703–706.
Hirschmann, M.M., 2010. Partial melt in the oceanic low velocity zone. Physics of the Earth and Planetary Interiors 179, 60–71.

Please cite this article in press as: Doglioni, C., et al., Tectonically asymmetric Earth: From net rotation to polarized westward drift of the lithosphere, Geoscience Frontiers (2014), http://dx.doi.org/10.1016/j.gsf.2014.02.001

Isacks, B., Molnar, P., 1971. Distribution of stresses in the descending lithosphere from a global survey of focal–mechanism solutions of mantle earthquakes. Reviews of Geophysics 9, 103–174.
Jeffreys, H., 1929. The Earth, second ed. Cambridge University Press, Cambridge.
Jin, Z.M., Green, H.G., Zhou, Y., 1994. Melt topology in partially molten mantle peridotite during ductile deformation. Nature 372, 164–167.
John, D.A., Ayuso, R.A., Barton, M.D., Blakely, R.J., Bodnar, R.J., Dilles, J.H., Gray, Floyd, Graybeal, F.T., Mars, J.C., M., D.K., Seal, R.R., Taylor, R.D., Vikre, P.G., 2010. Porphyry Copper Deposit Model. In: Chap. B of Mineral Deposit Models for Resource Assessment. U.S. Geological Survey Scientific Investigations. Report 2010–5070–B, 169 p.
Jordan, T.H., 1974. Some comments on tidal drag as a mechanism for driving plate motions. Journal of Geophysical Research 79, 2141–2142.
Jurdy, D.M., 1990. Reference frames for plate tectonics and uncertainties. Tectonophysics 182, 373–382.
Knopoff, L., Leeds, A., 1972. Lithospheric momenta and the deceleration of the Earth. Nature 237, 93–95.
Kreemer, C., 2009. Absolute plate motions constrained by shear wave splitting orientations with implications for hot spot motions and mantle flow. Journal of Geophysical Research 114. http://dx.doi.org/10.1029/2009JB006416.
Lallemand, S., Heuret, A., Boutelier, D., 2005. On the relationships between slab dip, back-arc stress, upper plate absolute motion, and crustal nature in subduction zones. Geochemistry, Geophysics, Geosystems 6. http://dx.doi.org/10.1029/2005GC000917.
Le Pichon, X., 1968. Sea-floor spreading and continental drift. Journal of Geophysical Research 73, 3661–3697.
Levin, B.W., Sasorova, E.V., 2012. Seismotectonics and Earth tides. Russian Journal of Pacific Geology 6, 70–77.
Ligi, M., Cuffaro, M., Chierici, F., Calafato, A., 2008. Three-dimensional passive mantle flow beneath midocean ridges: an analytical approach. Geophysical Journal International 175, 783–805.
Manea, V., Manea, M., Kostoglodov, V., Sewell, G., 2006. Intraslab seismicity and thermal stress in the subducted Cocos plate beneath central Mexico. Tectonophysics 420, 389–408.
Mitchell, A.H.G., Garson, M.S., 1981. Mineral Deposits and Global Tectonic Settings. Academic Press, London, UK.
Moore, G.W., 1973. Westward tidal lag as the driving force of plate tectonics. Geology 1, 99–100.
Moore, W.B., 2008. Heat transport in a convecting layer heated from within and below. Journal of Geophysical Research 113, B11407.
Morgan, W.J., 1971. Convection plumes in the lower mantle. Nature 230, 42–43.
Morgan, J.W., Phipps Morgan, J., 2007. Plate velocities in the hotspot reference frame. In: Foulger, G.R., Jurdy, D.M. (Eds.), Plates, Plumes, and Planetary Processes, Geol. Soc. Am. Spec. Pap., 430, pp. 65–78. http://dx.doi.org/10.1130/2007.2430(04).
Müller, R.D., Royer, J.Y., Lawver, L.A., 1993. Revised plate motions relative to the hotspots from combined Atlantic and Indian Ocean hotspot tracks. Geology 21, 275–278.
Naif, S., Key, K., Constable, S., Evans, R.L., 2013. Melt–rich channel observed at the lithosphere–asthenosphere boundary. Nature 495, 356–359.
Nelson, T.H., Temple, P.G., 1972. Mainstream mantle convection; a geologic analysis of plate motion. AAPG Bulletin 56 (2), 226–246.
Nishiwaki, C., Uyeda, S., 1983. Accretion tectonics and metallogenesis. In: Hashimoto, M., Uyeda, S. (Eds.), Accretion tectonics in the Circum-Pacific Regions: Proceedings of the Oji International Seminar on Accretion Tectonics, Japan, 1981, Advances in Earth and Planetary Sciences. Terra Scientific Publishing Company, Tokyo, Japan, pp. 349–355.
Norton, I.O., 2000. Global hotspot reference frames and plate motion. In: Richards, M.A., Gordon, R.G., der Hilst, R.D.V. (Eds.), The History and Dynamics of Global Plate Motions. Geophys. Monogr..
O'Connell, R.G., Gable, G.G., Hager, B.H., 1991. Toroidal-poloidal partitioning of lithospheric plate motion. In: Sabadini, R., L, K., Boschi, E. (Eds.), Glacial Isostaty, Sea-level and Mantle Rheology. Kluwer Acad. Publ..
Omori, S., Komabayashi, T., Maruyama, S., 2004. Dehydration and earthquakes in the subducting slab: empirical link in intermediate and deep seismic zones. Physics of the Earth and Planetary Interiors 146, 297311.
O'Neill, C., Müller, D., Steinberger, B., 2005. On the uncertainties in hot spot reconstructions and the significance of moving hot spot reference frames. Geochemistry, Geophysics, Geosystems 6.
Panza, G., Doglioni, C., Levshin, A., 2010. Asymmetric ocean basins. Geology 38, 59–62.
Pollack, H.N., Hurter, S.J., Johnson, J.R., 1993. Heat flow from the earth's interior: analysis of the global data set. Reviews of Geophysics 31, 267–280.
Pollitz, F.F., Brgmann, R., Romanowicz, B., 1998. Viscosity of oceanic asthenosphere inferred from remote triggering of earthquakes. Science 280, 1245–1249.
Presnall, D.C., Gudfinnsson, G.H., 2011. Oceanic volcanism from the low-velocity zone – without mantle plumes. Journal of Petrology 32, 1533–1546.
Ranalli, G., 2000. Westward drift of the lithosphere: not a result of rotational drag. Geophysical Journal International 141, 535–537.
Ricard, Y., Doglioni, C., Sabadini, C., 1991. Differential rotation between lithosphere and mantle: a consequence of lateral viscosity variations. Journal of Geophysical Research 96, 8407–8415.
Rietbrock, A., Waldhauser, F., 2004. A narrowly spaced double–seismic zone in the subducting Nazca plate. Geophysical Research Letters 31. http://dx.doi.org/10.1029/2004GL019610.
Riguzzi, F., Crespi, M., Cuffaro, M., Doglioni, C., Giannone, F., 2006. A model of plate motions. In: Sansò, F., Gil, J. (Eds.), Geodetic Deformation Monitoring: From Geophysical to Engineering Roles, International Association of Geodesy Symposia, vol. 131. Springer, pp. 200–208.
Riguzzi, F., Panza, G., Varga, P., Doglioni, C., 2010. Can earth's rotation and tidal despinning drive plate tectonics? Tectonophysics 484, 60–73.
Ritsema, J., Allen, R.M., 2003. The elusive mantle plume. Earth and Planetary Science Letters 207, 1–12.
Rychert, C.A., Laske, G., Harmon, N., Shearer, P.M., 2013. Seismic imaging of melt in a displaced Hawaiian plume. Nature Geoscience 6, 657–660.
Schmerr, N., 2012. The Gutenberg discontinuity: melt at the lithosphere-asthenosphere boundary. Science 335, 14801483.
Scoppola, B., Boccaletti, D., Bevis, M., Carminati, E., Doglioni, C., 2006. The westward drift of the lithosphere: a rotational drag? Geological Society of America Bulletin 118.
Shapiro, N.M., Ritzwoller, M.H., 2002. Monte-Carlo inversion for a global shear-velocity model of the crust and upper mantle. Geophysical Journal International 151, 88–105.
Shapiro, N.M., Ritzwoller, M.H., 2004. Inferring surface heat flux distributions guided by a global seismic model: particular application to Antarctica. Earth and Planetary Science Letters 223, 213–224.
Shaw, H.R., 1973. Mantle convection and volcanic periodicity in the Pacific: evidence from Hawaii. Geological Society of America Bulletin 84, 1505–1526.
Silver, P.G., Beck, S.L., Wallace, T.C., Meade, C., Myers, S.C., James, D.E., Kuehnel, R., 1995. Rupture characteristics of the deep Bolivian earthquake of 9 June 1994 and the mechanism of deepfocus earthquakes. Science 268, 69–73.
Smith, D.E., Kolenkiewicz, R., Dunn, P., Robbins, J.W., Torrence, M.H., Klosko, S.M., Williamson, R.G., Pavlis, E.C., Douglas, N.B., Fricke, S.K., 1990. Tectonic motion and deformation from satellite laser ranging to LAGEOS. Journal of Geophysical Research 95, 23013–22041.
Solomon, S.C., Sleep, N.H., 1974. Some simple physical models for absolute plate motions. Journal of Geophysical Research 79, 2557–2567.
Steinberger, B., Sutherland, R., O'Connell, R.J., 2004. Prediction of Emperor-Hawaii seamount locations from a revised model of global plate motion and mantle flow. Nature 430, 167–173.
Storchak, D., Di Giacomo, D., Bondár, I., Harris, J., 2012. ISC-GEM: Global Instrumental Earthquake Catalogue (1900–2009). In: AGU Fall Meeting. San-Francisco, USA.
Tackley, P.J., 2000a. Mantle convection and plate tectonics: toward an integrated physical and chemical theory. Science 288, 2002–2007.
Tackley, P.J., 2000b. Self consistent generation of tectonic plates in time-dependent, three dimensional mantle convection simulations: 1, pseudoplastic yieldings. Geochemistry, Geophysics, Geosystems 1, 2000GC000036.
Thybo, H., 2006. The heterogeneous upper mantle low velocity zone. Tectonophysics 416, 53–79.
Torsvik, T.H., Steinberger, B., Gurnis, M., Gaina, C., 2010. Plate tectonics and net lithosphere rotation over the past 150 my. Earth and Planetary Science Letters 291, 106112.
Trampert, J., Deschamps, F., Resovsky, J., Yuen, D., 2004. Probabilistic tomography maps chemical heterogeneities throughout the lower mantle. Science 306, 853–856.
Turcotte, D.L., Schubert, G., 2002. Geodynamics, Application of Continuum Physics to Geological Problems, second ed. John Wiley & Sons, New York.
Uyeda, S., Kanamori, H., 1979. Back-arc opening and the mode of subduction. Journal of Geophysical Research 84, 1049–1061.
Varga, P., Krumm, F., Riguzzi, F., Doglioni, C., Süle, B., Wang, K., Panza, G.F., 2012. Global pattern of earthquakes and seismic energy distributions: insights for the mechanisms of plate tectonics. Tectonophysics 530, 80–86.
Vassiliou, M.S., Hager, B.H., 1988. Subduction zone earthquakes and stress in slabs. Pure and Applied Geophysics 128, 547–624.
Vérard, C., Hochard, C., Stampfli, G., 2012. Non-random distribution of euler poles: is plate tectonics subject to rotational effects? Terra Nova 24 (6), 467–476. http://dx.doi.org/10.1111/j.1365-3121.2012.01085.x.
Wang, S., Wang, R., 2001. Current plate velocities relative to hotspots: implications for hotspot motion, mantle viscosity and global reference frame. Earth and Planetary Science Letters 189, 133–140.
Wessel, P., Smith, W.H.F., 1995. New version of Generic Mapping Tools (GMT) version 3.0 released. Eos, Transactions American Geophysical Union 76, 329–329.
Wilson, J.T., 1973. Mantle plumes and plate motions. Tectonophysics 19, 149–164.
Zheng, L., Gordon, R.G., Argus, D., DeMets, C., Kreemer, C.W., 2010. Current plate motion relative to the hotspots and to the mantle. In: Abstract GP24A-07 Presented at 2010 Fall Meeting, AGU, San Francisco, Calif., 1317 Dec.
Zhong, S., 2001. Role of ocean-continent contrast and continental keels on plate motion, net–rotation of the lithosphere and the geoid. Journal of Geophysical Research 106, 703–712.

Please cite this article in press as: Doglioni, C., et al., Tectonically asymmetric Earth: From net rotation to polarized westward drift of the lithosphere, Geoscience Frontiers (2014), http://dx.doi.org/10.1016/j.gsf.2014.02.001